SIMULATION ANALYSIS AND EXPERIMENTAL VALIDATION OF ULTRASOUND ENERGY TRANSFER IN THE NEAR FIELD TO CHARGE MEDICAL IMPLANTS

By

AMMAR A. MOHAMMED

A dissertation submitted in partial fulfillment of
the requirements for the degree of

DOCTOR OF PHILOSOPHY

WASHINGTON STATE UNIVERSITY
School of Mechanical and Materials Engineering

MAY 2021

To the Faculty of Washington State University:

The members of the Committee appointed to examine the dissertation of AMMAR A. MOHAMMED find it satisfactory and recommend that it be accepted.

_____

Changki Mo, Ph.D., Chair

_____

John Miller, Ph.D., Co-Chair

_____

Joseph Iannelli, Ph.D.

_____

David Lowry, Ph.D.

ACKNOWLEDGMENT

I would like to thank Dr. Changki Mo (Chair), Dr. John Miller (Co-Chair), Dr. David Lowry, and Dr. Joseph Iannelli for their guidance and support. I would like to acknowledge and thank my family for supporting me and for the landlord of the house who helps me and let me use my experimental instrument inside his house due to COVID-19. I appreciated each professor separately and would like to write a new acknowledgment for each one. My committee chair and advisor, Dr. Mo, extremely supported me with the idea for the project and the guidance. Dr. Mo helped me in every step and he instructed every part of my dissertation and research. Without his help, this project would not have been possible for me to complete.

I also can't forget how Dr. Miller helped me and gave me his valuable time to explain machine learning, neural network, and finally data mining. I can't forget how Dr. Lowry taught me electromagnetics to help pursue my dissertation.

I would like to thank Dr. Joseph Iannelli for his nice smile every time that he sees me. I still remember how he supported my project in the preliminary exam with his nice words, which made me feel relax and reduced my anxiety.

SIMULATION ANALYSIS AND EXPERIMENTAL VALIDATION OF ULTRASOUND ENERGY TRANSFER IN THE NEAR FIELD TO CHARGE MEDICAL IMPLANTS

Abstract

by Ammar A Mohammed, Ph.D.
Washington State University
May 2021

Chair: Changki Mo
Co-Chair: John Miller

Acoustic power transfer technology is a method for wirelessly energy transfer to implantable medical devices. The advantage of ultrasonic power transfer over inductive power transfer is the longer-distance range between the transmitter and receiver. Inductive power transfer is more powerful and even has high efficiency if the distance is in the order of the transmitter diameter or less. Nevertheless, in some cases short-distance ultrasonic power transfer may be employed; consequently, their operation may be complicated by the near-field aspects of piezoelectric acoustic energy transfer. Rapidly varying characteristics of the near-field region present challenges to experimental investigation.

A piezoelectric energy transfer system consisting of two lead zirconate titanate (PZT) transducers was analyzed and tested, focusing on the near-field in this work. To facilitate this study, simulation analysis was used to investigate the effects on the voltage output of simultaneous variations of multiple pairs of physical parameters, such as changing the diameters of both receiver and

transmitter. These physical parameters were used to model, analyze, and simulate the performance of a piezoelectric ultrasonic energy transfer system using COMSOL Multiphysics software then validate experimentally. Moreover, the effect of the thickness ratio and diameter ratio on the power transfer efficiency was observed to be significant when the transmitter thickness was 1 mm. The simulation results indicated that changing multiple parameters simultaneously was more effective for energy transfer than changing individual parameters. The effects of operating frequency on power transfer efficiency at various distances between transmitter and receiver were also studied. It was found that the frequencies below 1 MHz showed almost zero power transfer efficiency regardless of the distance between two PZT transducers. The rotation angle that represents the misalignment between the PZT receiver and transmitter can make the power transfer efficiency change significantly by a few degrees. Finally, reflector layer effects on power transfer efficiency were investigated through simulation analysis. The simulation results indicated that the reflector layer can improve power transfer efficiency depending on its material, dimension, and location.

TABLE OF CONTENTS

Page

LIST OF TABLES

Page

LIST OF FIGURES

Page

Dedication

For my parents

CHAPTER ONE: Introduction

Implantable medical devices are used to replace or assist organs in the human body. When batteries of the implantable device are running out of power, replacement surgery is required. This disadvantage of batteries leads researchers to find a new way to supply energy for the implantable device. One of these methods is transferring energy by using ultrasound. The wireless piezoelectric ultrasonic system can provide long-term, stable, and efficient electric energy for implantable devices. The system can transmit electric power from the power sources to the loads in a wireless way. Wireless power transfer usually requires a good alignment between piezoelectric transmitter and receiver and suffers from a drastic loss of efficiency when transmission depth increases. Most researchers recommend using a frequency lower than 20 MHZ to avoid tissue heating [1]. To maintain an excellent transferring efficiency, two PZT (lead zirconate titanate) transducers must have the same resonant frequency and have a small transmission depth.

1.1 PZT transducer sending and receiving electric circuit

The implantable medical device consists of a pair of piezoelectric transducers acting as a transmitter-receiver system. The system was equivalent to an electric circuit represented by Krimholtz et al. [2]. The source of the electric system is an AC signal (V_{in}) that makes the PZT transducer vibrate at a certain frequency mode called thickness-expansion mode. The PZT discs have C_t and C_r as capacitive devices for transmitter and receiver, respectively. X_t and X_r represent the transducer impedance at which the frequency vanishes. The transmission efficiency can be increased by setting the X_r equal to zero that can happen when the operation frequency is set to be the same as the PZT receiver natural frequency. (1: Φ) represents the electromechanical coupling that is modeled as a transformer. The mass of the two faces for each PZT are modeled as

transmission line with impedance (Z_t, Z_r). The electrical load signal is V_l. The resonant frequency (f_r) is the frequency of the sound wave in the material (traveling velocity in the piezoelectric material) to that material thickness (t). The lowest thickness mode frequency of mechanical vibration is such that the disc is half a wavelength thick [3].

$$T = \frac{\lambda}{2} = \frac{c}{2f_r} \qquad f_r = \frac{c}{2T} \tag{1}$$

where λ is the wavelength of the resonant mode. T is the thickness of a piezoelectric disc. c is the longitudinal wave velocity in the piezoelectric material, f_r is the fundamental resonance frequency. The equation (1) can be written in the following form.

$$f_r = \frac{V_D}{2 \times t} \tag{2}$$

Where, v_D is the traveling velocity in the piezoelectric material. The ultrasonic transducer usually consists of three layers: a piezoelectric layer, an impedance matching layer, and a backing layer. The backing layer absorbs the ultrasound on the backside [4].

1.2 Motivation

The implantable medical device (IMD) has been investigated since the late 1950s [5]. The first report about an electrical heart stimulator was by P. Zoll in 1952. The invention of lithium-metal batteries in the early 1970s opened up the possibility of powering implantable devices [6]. Antonioli et al. [7] invented the first pacemaker powered by lithium cell. An ultrasonically power transfer device was developed by Phillips et al. [8] in 2003, but many IMD like artificial kidneys still use wires to power the implantable devices.

The following reasons to use an ultrasound transfer power instead of wires in supplying IMD are discussed in the next section:

A. Patient facing difficulties to move normally.
B. Wires coming out from the skin can be a major source of infection.
C. The battery has limited life and needs replacement.
D. The size of IMD's battery can be smaller.
E. Safe powering conditions.

1.3 Discussion

A. Patient facing difficulties to move normally: Some device like wearable artificial kidney already attached to a special jacket. The jacket with the device will be heavy causing the patient movement to be difficult, especially for senior people.
B. Wires coming out from the skin can be a major source of infection: When the patient moves the wire keeps vibrating inside the skin of the human body due to the muscle movement. Then blood will come to cause the area to be at the risk of infection.
C. The battery has limited life and needs replacement: There are many types of battery each of which works for a certain lifetime and provides different power. These batteries are lithium batteries, bio-fuel cells, nuclear batteries, thermoelectricity, piezoelectricity, electromagnetic generators, optical charging, ultrasonic transducer, and inductive coupling. Basaeri et al. [9] presented that the bio-implantable device could be used for therapeutic functions as well as collecting data for scientific studies. For implantable devices batteries are an important part to achieve continuous operation. The supply power has problematic in many of these devices because of the limited lifetime and the size of the batteries.
D. The size of IMD's battery can be smaller: Normally the size of an implantable device is very important because it is inside the human body. The battery takes most space of IMD

size. The battery size could be large to provide a longer lifetime. However, supply power by using ultrasound can help to minimize the battery size, charging wirelessly.

E. Safe powering conditions: Using ultrasonic power transfer is considered safe and effective [10]. Even the batteries attached to IMD still appear to be safe. Awal et al. [11] mentioned that acoustic energy transfer is the safest and a high-performance method to transfer energy to the inside human body (to an implanted medical device) than electromagnetic or microwave. The authors found that Mason (1948) provided an equivalent circuit for piezoelectric, which is still widely used. Typically, IMD requires little power to operate, normally within mW. Many researchers focus on maximizing power. The maximum power transfer they presented was 5.4 W, making the efficiency 36%.

1.4 Objectives

1. Perform comprehensive parametric study for an ultrasonic power transfer system to investigate the effect of depth, diameter, thickness, and rotation angle on power transfer efficiency.
2. Investigate the highest transfer power efficiency related to the system's preferred location in the near-field region. Looking into the effect of the acoustic pressure, sound pressure level, and radiation pattern provides the insight to find this location.
3. Find the optimal operation condition by choosing the parameters selected for high efficiency in steps 1 and 2, then using multiple locations, and thickness for a reflector to increase the power transfer efficiency.

1.5 Problem statement

In 2018, more than 200 Canadians died while waiting for organ transplants [12]. This problem opens the way for implantable medical devices to replace the organs with an artificial one. The main problem with long-term use is power because the battery has a certain lifetime. The researchers tried to use power transfer so that they started with transformers where the skin is the medium and ended with an ultrasound PZT system (a safe method to transfer the energy). The ultrasonic coupling wireless power transfer is a non-contact energy transmission method that uses ultrasonic waves as a carrier to convert electrical energy into acoustic energy through electro-acoustic conversion materials and convert the acoustic energy into electrical energy through acoustic-electric conversion materials. This dissertation was performed to check whether it is possible to develop such a system to work with a different part of the human body that required a high power transfer efficiency for example the kidney. Also, an attempt has been made to create an experimental and simulated system to evaluates the parameters that can affect the ultrasonic waves that power and control implantable devices.

1.6 Dissertation outline

This dissertation consists of seven chapters summarized as follows. Chapter two comprises a literature review on the subject of implanted medical devices and ultrasound energy transfer between two PZTs, the transmitter, and receiver. Chapter three covers the methodology of present simulation results done by using COMSOL software and experimental validation. Chapter four focuses on the power transfer between the PZT-5H transducers. The factors that affect the system energy transmissibility were studied, considering alignment and distance between the PZT receiver and transmitter. Chapter five studies the power transfer efficiency between the different

sizes of a new modified PZT-4 to find the optimal PZT system efficiency between different PZT size. The diameter, size, and thickness will be different. Chapter six deals with the reflector layer and its location to optimize the system. Chapter seven contains the conclusion and recommendation.

1.7 Contribution

- Analyze the effects of changing the parameters to find the optimal boundary condition for the medical implantable device so the device can work with different parts of the human body that required certain power.
- Extensively evaluate the influence of various application parameters, such as orientation, on acoustic power transfer between two circular-shaped transducers with a short distance between the piezoelectrics.
- The effects of simultaneous variations of multiple pairs of physical parameters, such as changing the diameter of the receiver and transmitter simultaneously or the effect of changing the depth and thickness simultaneously on the power transfer efficiency are investigated.

1.8 State of the art

In recent years, the interest in medical devices that function inside the human body has increased. Instruments for sensing and controlling the specific functions of the human body have increased due to the technological advancement of electronics and the increased efficiency of powering the system [13]. Wireless power transfer (WPT) is a new safety technology that provides electrical voltage to the implantable medical device without using electrical wires or batteries (compared to

other methods) that can cause disease. To avoid any disease, the medical device should be made from biocompatible materials [14]. The main advantage of WPT is that the patient is not required to be linked to a certain location by cables. The development of IMD in a biological system made it easier to use with a different part of the human body, such as biological sensors, pacemakers, cardiac defibrillators, and deep brain stimulators, etc. WPT can be used for both wearable and implantable applications such as deep brain stimulation. IMD should have packaging to isolate it from body tissue [15]. IMD must satisfy two issues: first, to be biocompatible with the human body and second, the receiver should have efficient transforms.

In 1914, Telsa proved that WPT is a possible method of future wireless powering [16]. In 1921, Tesla showed that the capacitive powering system will wirelessly turn on an electric bulb between two capacitor plates [16]. After 1980, the WPT started to experience its anticipated growth as wireless communication. In 1985 [17] acoustic energy was transferred wirelessly to a fixed plate inside the body to treat a bone. Since 2000, the development of WPT has become serious research [18].

The first demonstration of the piezoelectricity was by Jacques in 1880 [20] who showed electricity generation by applied stress. Gabriel in 1881 confirmed the converse effect of piezoelectricity [19]. In 1997 Connor demonstrated power transfer between two piezoelectric transducers attached face-to-face with a solid wall between them as a medium [20].

1.9 References

1. Sauer, C., Stanacevic, M., Cauwenberghs, G., & Thakor, N. (2005). Power harvesting and telemetry in CMOS for implanted devices. IEEE Transactions on Circuits and Systems I: Regular Papers, 52(12), 2605-2613.

2. Krimholtz, R., Leedom, D. A., & Matthaei, G. L. (1970). New equivalent circuits for elementary piezoelectric transducers. Electronics Letters, 6(13), 398-399.

3. Guo, N. (1989). The vibration characteristics of piezoelectric discs (Doctoral dissertation, University of London).

4. Azhari, H. (2010). Basics of biomedical ultrasound for engineers. John Wiley & Sons.

5. Zhou, J. (2019). Ultrasonically Controlled/Powered Implantable Medical Devices (Doctoral dissertation, Purdue University Graduate School).

6. Schneider, A. A., & Moser, J. R. (1972). U.S. Patent No. 3,674,562. Washington, DC: U.S. Patent and Trademark Office.

7. Antonioli, G., Consiglio, F., Lebrun, R., Baggioni, F., Grassi, G., & Zanardi, F. (1973). Implantable cardiac stimulator with a new solid-state lithium battery. Minerva medica, 64(43), 2298-2304.

8. Phillips, W. B., Towe, B. C., & Larson, P. J. (2003, September). An ultrasonically-driven piezoelectric neural stimulator. In Proceedings of the 25th Annual International Conference of the IEEE Engineering in Medicine and Biology Society (IEEE Cat. No. 03CH37439) (Vol. 2, pp. 1983-1986). IEEE.

9. Basaeri, H., Christensen, D. B., & Roundy, S. (2016). A review of acoustic power transfer for bio-medical implants. Smart Materials and Structures, 25(12), 123001.

10. Amar, A. B., Kouki, A. B., & Cao, H. (2015). Power approaches for implantable medical devices. sensors, 15(11), 28889-28914.

11. Awal, M. R., Jusoh, M., Sabapathy, T., Kamarudin, M. R., & Rahim, R. A. (2016). State-of-the-art developments of acoustic energy transfer. International Journal of Antennas and Propagation, 2016.

12. https://globalnews.ca/news/6253000/canada-organ-donation-supply/

13. Ikeda, K., Doi, M., Kazama, T., Sato, K., & Oyama, T. (Eds.). (2012). Computing and monitoring in anesthesia and intensive care: recent technological advances. Springer Science & Business Media.

14. Haerinia, M. (2020). A State of Art Review on Wireless Power Transmission Approaches for Implantable Medical Devices. arXiv preprint arXiv:2003.01240.

15. Joung YH. Development of implantable medical devices: from an engineering perspective. Int Neurourol J Sep 2013;17(3):98–106.

16. Tesla, N. (1914). U.S. Patent No. 1,119,732. Washington, DC: U.S. Patent and Trademark Office.

17. Roes, M. G. L. (2015). Exploring the potential of acoustic energy transfer [Ph. D. dissertation]. Technische Universiteit Eindhoven, Eindhoven, The Netherlands.

18. Tesla, Experiments with Alternate Currents of Very HighFrequency and their Application to Methods of Artificial Illumination, Wilder, Radford, Va, USA, 2008.

19. Jacques, C., & Pierre, C. (1880). Development, via compression, of electric polarization in hemihedral crystals with inclined faces. Bull. Soc. Minérologique Fr, 3, 90-3.

20. Connor, D. J., Cummings, G. F., & Star, M. J. (1997). U.S. Patent No. 5,594,705. Washington, DC: U.S. Patent and Trademark Office.

CHAPTER TWO: Literature review

2.1 Introduction

There is an enormous increase in the number of medical implantable devices. Most of these devices require power for their operation [1]. In this dissertation, ultrasonic waves are going to be analyzed to power and control implantable devices. Ultrasonic coupling systems have a pair of transducer, transmitter, and receiver. AC signal causes the piezoelectric transducer to vibrate at a frequency ($\geq$ 1 MHz). The transducer undergoes a vibration mode called thickness-expansion mode. When the PZT element operates at its natural frequency a high transmission efficiency will result.

Basaeri et al. [2] found that the harvested energy available inside the human body is generally not sufficient to power implanted devices. To charge these batteries acoustic power transfer method was proposed. Acoustic power, emitted from a piezoelectric transmitter (TX), is in contact with the skin is transmitted as waves. TX is vibrating due to alternating electric voltage connected to the PZT so the PZT vibration generates continuous acoustic waves these waves are capable of transferring through gases, liquids, and solids. This pressure wave will hit the receiver piezoelectric (RX) and shake it causing stress in the material to induce a voltage, as illustrated in figure 1.

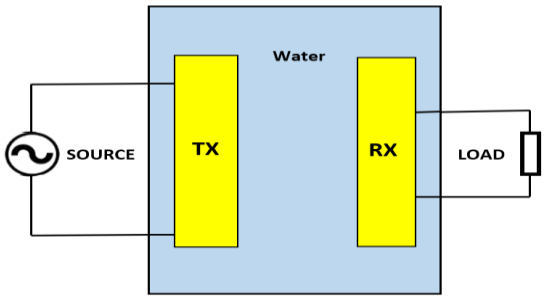

Figure 1: Schematic of the main components of a PZT system, where TX and RX denote PZT receiver and transmitter, respectively.

2.2 Wave Equation

The wave equation that represents the linear acoustic under the assumption of an isentropic equation is illustrated in equation (3).

$$\frac{1}{c^2}\frac{\partial^2 p}{\partial t^2} = \nabla^2 p = 0 \tag{3}$$

Where c is the isentropic speed of the sound and p is the acoustic pressure. The pressure $p(x, t)$, can be derived as a function of the acoustic particle velocity, $u(x, t)$ along the x-axis.

$$p(x,t) = \rho c u(x,t) \tag{4}$$

ρ is the density of the medium and $z = \rho c$ the acoustic impedance of the medium. The SI unit of acoustic impedance is Pa.s.m^{-1}, often called the rayl.

The acoustic impedance refers to how much pressure is generated by the vibration of the medium at the desired frequency. The acoustic pressure properties change in the medium and are commonly split into near-field and far-field affects. In the near-field, the emission of the wave is cylindrical and has many minima and maxima values, while in the far-field the transmission of the wave is spherical and its decay with the distance. The reflection coefficient is defined by.

$$\Gamma = \frac{z_2 - z_1}{z_2 + z_1} = \frac{p_r}{p_i} \tag{5}$$

Where z_1 is the transducer acoustic impedance, z_2 medium impedance, p_r the amplitude of reflection wave, p_i the amplitude of the incident wave. Equation (5) shows that with the larger reflection value, a little wave will be the recipient (when Γ is high p_i is small). Another concern about the mismatch is the pressure standing wave that can generate peak pressure levels that exceed

the safety of tissue. However, the matching impedance can be calculated for the following equation.

$$z_{matching} = \sqrt{z_1 \cdot z_2} \tag{6}$$

The acoustic impedance of the receiver can be adjusted by using a resistor that can be added to the PZT receiver. At the same time, the FDA (Food and Drug Administration) mentioned that the intensity of the system should not exceed the 7200 $\mu W/mm^2$ to avoid skin damage.

Huygens principle is a method for calculating the acoustic pressure at a location away from the transducer. Each vibrating point on the surface of the transmitter can be considered as the center of a new point source emitting acoustic waves. Assuming a circular piston transmitter of radius a, the increment area is ds, the distance to the observation point is *l*, *f* is the frequency and *u* is particle velocity at ds as illustrated in figure 2, the acoustic pressure for circular PZT can be calculated from the equations (7) and (8).

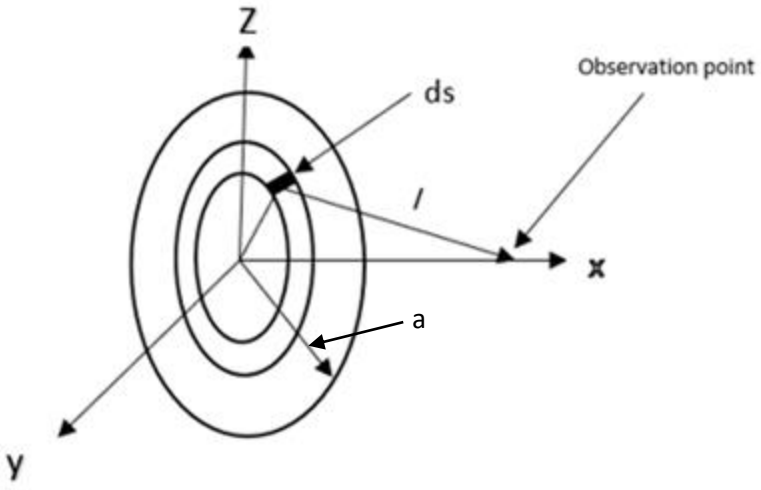

Figure 2: Transmitter geometry.

$$p = -j\rho_0 uf \int_0^{2\pi} \int_0^a \frac{e^{j\frac{\omega}{c_0}(l-c_0 t)}}{l} r dr d\varphi \tag{7}$$

$$l = \sqrt{r^2 + x^2} \tag{8}$$

The best efficiency is when TX and RX have the same size, but sometimes the application required different sizes. In case TX diameter is greater than RX diameter, the receiver may not capture all the acoustic waves transmitted by TX. The efficiency will be low, and the intensity could still be high.

Mo et al. [3] calculated the power transmission of the ultrasound PZT that could recharge the system of an implantable medical device. The system efficiency depends on the frequenceies of the TX and RX, mechanical acoustical impedance, and the distance between the transducers of the system as well as the misalignment. The sensitivity of the alignment of transducers was investigated by using finite-difference time-domain (FDTD) simulation. The results showed how the acoustic pressure variation versus axial distance. The authors clearly showed that variations in the acoustic pressure field in the near field region are significant because the field goes through a series of peaks and nulls. The authors reported that near-field distance from the transducer depends on the transducer's radius and the acoustic wavelength in the medium through which the wave propagates.

Mo et al. [3] showed that the receiver should be positioned at a point along the path of the sound wave. The near- and far-field regions of an ultrasound power transfer system are illustrated in Figure 3.

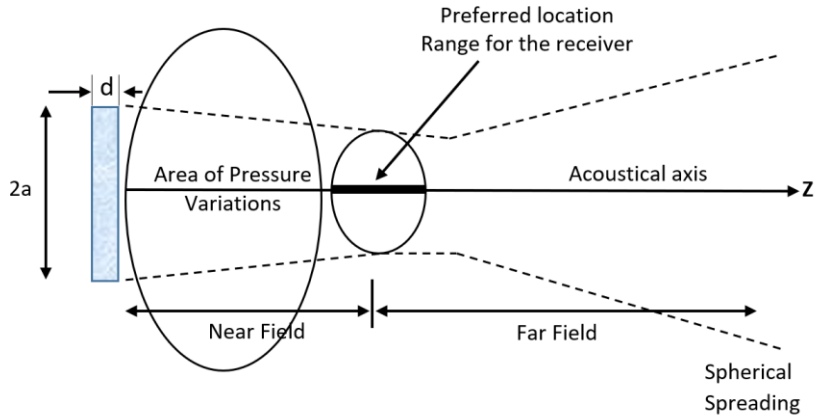

Figure 3: Near- and far-field locations for a receiver relative to the transmitter of a PZT system.

The far-field region starts beyond the zone of the natural focus where the pressure field becomes a spherically spreading wave with little internal structure and whose intensity decays with distance. In this dissertation, we report of the key design parameters that influence output voltage in the near-filed region and optimize them using the COMSOL software package [11]. Model predictions are validated by experimental measurements.

2.3 PZT alignment

Christensen et al. [4] found that the PZT receiver implanted in biological tissue is difficult to stabilize. When the receiver position is not fixed, slight variations in depth, orientation, and alignment, which define the spatial relationship between RX and TX, can cause significant variations in the transferred power. Christensen et al. [4] placed the receiver and transmitter PZT in an acoustic test tank. RX PZT load voltage had 2 Ω resistance while the PZT transmitter had a resistor of 986 Ω. The voltage source is 16 V at frequency 1 MHz. The measurements between the PZT TX and RX were 12.5 to16 mm in increments of 0.1 mm at 0° angle and 0 mm offset. The angle measurements were taken from (−45° to 45°) in increments of 1°.

2.4 Power transfer efficiency

Ozeri and Shmilovitz [5] proposed an ultrasonic transcutaneous energy transfer (UTET) device that can transfer the energy by the acoustic wave. UTET device can be affected by certain parameters, including amplifier loss, transducer losses, tissue absorption, acoustic impedance matching layer losses, rectifier losses, and the amount of power captured by the receiver. The acoustic impedance of PZT is higher than the medium (tissue) so acoustic impedance matching is required. Matching acoustic impedance will minimize the pressure wave reflections and prevent the standing wave. The finite element simulation of one transducer was generated. The pressure intensity in the paper shows the directivity of the radiated pressure wave.

The transducer operated close to its natural frequency to maximize the power throughput of the transducer. The traducer resonance frequency can be calculated from the following equation where N_t is the speed of sound of the piezoelectric material, and t is the PZT thickness.

$$f_r[Hz] = \frac{N_t}{t} \tag{9}$$

The authors tested an implanted device located at 40 mm depth with 70 mW. The results showed that the distance and relative orientation, as the tissue moves or deform, affected the system efficiency. These authors also mention that the skin and underlying soft tissue layer have acoustic impedance and phase velocities that are close to those of water. The acoustic impedance refers to the pressure generated by the vibration of the medium at the desired frequency [6]. The transducer impedance should match tissue impedance to avoid reflected pressure waves.

Ozeri et al. [7] used a PZT transmitter constructed of six concentric elements (six equal areas where the electrode is partitioned) and each element connected to a separate excitation source. The excitation voltage generates a continuous wave. The frequency of the system is 650 kHz. This

frequency can be received by a PZT receiver that has a thickness of less than 5mm including the matching layer. These sources will excite all the PZT elements uniformly leading to a uniform surface vibration amplitude. These transmitters have a self-natural focusing zone, and each element can be operated by its voltage source with a unique amplitude level. A disadvantage is the presence of in side-lobes, which tend to decrease the amount of energy harvested by the receiver.

This PZT powered a device implanted 50mm deep inside the human body. The entire system was submerged inside the aquarium and covered by an ultrasound absorber sheet to avoid reflection. Distilled water is used as a medium for acoustic wave pressure measurements because its acoustic impedance is close to that of soft biological tissue. The skin and the underlying soft tissue layer have acoustic impedances and phase velocities that are close to those of distilled water.

2.5 Power transfer focusing

Gorostiaga et al. [8] showed that the electrical load should match the impedance of the transmission medium to achieve zero reflection coefficient so that all of the power of the incoming wave is transmitted to the PZT receiver, and that the frequency of operation should be adjusted depending on acoustic radiation and pressure distribution to get efficient power transfer.

Lee et al. [9] showed that magnetic resonance and induction coupling are techniques to transfer the energy a short distance; hence, they can only supply medically implanted devices close to the human skin. The ultrasound resonance method is a newly proposed IMD which successfully transfers power to an adjustable distance between the PZT TX and RX. The preferred location of PZT RX depends on the frequency of the system and the diameter of TX. Axial sound pressure can be calculated for the following equation.

$$p(r,0,t) = \rho_0 c U_0 e^{-\alpha r}\{1 - e^{-jk(\sqrt{r^2+a^2}-r)}\}e^{j(\omega t - kr)} \quad (10)$$

Table 1: Sound pressure equation variable.

ρ_0	Density of the medium	c	Sound speed in the medium
U_0	Velocity of the piston source of the transmitter	α	Attenuation coefficient
ω	Angular velocity	$k = \frac{\omega}{c}$	Wavenumber
r	Distance from the transmitter	a_{TX}	Radius of the transmitter
a_{RX},	Radium of receiver		

The electrical voltage of the transmitter and the input electrical power can be calculated from

$$P_{input} = \frac{V_{rms}^2}{Z_{TX}} \tag{11}$$

where V_{rms} is applied RMS voltage, and Z_{TX} is the impedance of the transmitter.

The total acoustic output power is defined as.

$$P_{acoustic} = [\int P_{rms} dA]^2 / [\int \rho c dA] \tag{12}$$

Wireless power transfer efficiency can be calculated from the following equations: The power conversion ratio between input electrical power and output acoustic power is

$$\eta_{EA} = {P_{acoustic}}/{P_{input}} \tag{13}$$

The output power is, $$P_{output} = \frac{V_{rms}^2}{R} \tag{14}$$

Where R equals the internal resistor of the receiver device. The power conversion ratio between input acoustic power and output electrical power is,

$$\eta_{AE} = {P_{output}}/{P_{acoustic}} \quad (15)$$

Total wireless power transfer efficiency is,

$$\eta_{all} = {\eta_{EA}}/{\eta_{AE}} \quad (16)$$

Saat et al. [10] used these equations to calculate the power transfer efficiency of a PZT system with air and metal block as a transfer medium.

Shaul et al. [12] mentioned that many implanted devices required electrical energy for operation. The authors showed that the power transfer from outside to inside the human body is very sensitive to skin-depth, but it can be controlled by a feedback circuit that has a backward data link. The simulation was achieved by exciting an external coil attached to the skin with an AC source (0.01 A). The results showed that to capture most of the acoustic power transfer, the transducer should be on the acoustic axis to meet the main pressure loop.

Silveira et al. [13] found a procedure to reduce the back-lobe level of a linear microstrip antenna arrays by designing radiators asymmetrically positioned with respect to the ground plane. This work was validated by designing a four-element linearly polarized array with half-wavelength spacing assisted by HFSS software. The authors showed that by changing the location and dimensions of the arrays, the back lobe can be suppressed.

2.6 Some implanted device application

Maleki et al. [14] present an implanted micro-oxygen generator device (IMOG) that is powered by ultrasonic waves. Oxygen is generated through water electrolysis and hydrogen is eliminated through the lungs. The authors plot the relationship between the electric current vs voltage generated and distance vs voltage generated (voltage drops exponentially with distance) at IMOG. The maximum current (400 μA) appears at 2.3 MHz (the resonance frequency of the PZT).

Power transfer efficiency (PTE), the ratio of power delivered to the load to that emitted from the source, is the key to evaluate the performance of the wireless link [15]. To increase PTE a resonant tuning frequency needs to be used. Also using a passive network matching technique can optimize the load resistance value to achieve maximum PTE. To carry energy wirelessly, the ultrasonic energy transfer wave should have a frequency larger than 20 kHz. Each point on the PZT transmitter could be considered as an independent source of radiation, so the acoustic field pattern can be the sum vector of all these points. Increased skin depth can be compensated by changing the system frequency and as a result, the power transfer efficiency, and that will affect the battery life. PTE is affected by many factors such as transducer losses (side lobe losses), RX absorption losses, tissue absorption, impedance matching-layer losses. When the pressure wave moves from TX to RX, it will encounter acoustic impedance mismatches so part of the wave will be reflected from TX and tissue boundaries. The formula that represents the reflection coefficient is $|\tau| = \left|\frac{z_{tissue}-z_{pzt}}{z_{tissue}+z_{pzt}}\right|$. To achieve optimal operating frequency the following factors need to be considered: transducer material, location of skin depth, TX or RX acoustic matching impedance, tissue growth, hydration or ambient temperature, different organs have different densities, acoustic impedances, type of tissue layer, directivity and PZT efficiency. Since the PZT-TX is outside the human body,

it can be larger compare to the implanted one with size limitation because of the space inside the body. For high gain, high directivity and efficiency needs to be achieved.

Approximately 2 million people in the world are receiving treatment for renal disease. A wearable blood-based renal device was created by Salani et al. [23]. This wearable artificial kidney can be inserted inside the human body. It is powered by 9 V and AA batteries. The battery could be replaced with an implantable PZT system.

An implantable artificial kidney, developed by H. David Humes at the University of Michigan, is currently undergoing preclinical studies.

Mahmood et al. [24] designed an ultra power transfer system. The transmitter side has a function generator and a TX sensor while the receiver side has the RX sensor, bridge rectifier, boost converter, and super-capacitor. The authors show how output power and transfer efficiencies, defined by equation (17), depend on the PZT skin-depth (separation of TX and RX).

$$Transfer\ Efficiency\ \%\ (\eta) = \frac{Output\ Power}{Input\ Power} \times 100\% \tag{17}$$

Zaid et al. [25] discuss how PZT acoustic energy transfer is affected by attenuation, diffraction, and reflection in the medium. Diffraction occurs when the wave encounters an obstacle so the wave has to bend and spread out. Reflections can be avoided by using a good match of impedance between the medium and the PZT. Material acoustic impedance should be involved in determining the medium of transmission because it specifies how much sound pressure that a certain frequency generates. The acoustic impedance can be calculated by multiplying the medium density and the propagation velocity of sound in the material. Zaid et al. [25] showed that the resonance frequency of the system should match with the transducer's frequency to get the highest energy transfer. The relation between power output and the air gap was investigated by simulating a PZT with perfect

alignment. As expected, an increase in the gap leads to a decrease in power. Zaid et al. [25] also investigated the use of multiple transducers in one system. This type of multiple PZT will make the power transfer higher than a single one where each transducer is connected to the other in parallel. The authors present the effect of multiple transducers as a function for the output power and slow that increasing the number of traducers achieves better power transfer.

Kar et al. [26] studied the power transfer through two different media, aluminum, and polyoxymethylene (POM) with contrasting specific acoustic elements. They found the most important factors that can affect the energy transfer are (1) properties of the piezoceramic material, (2) the acoustic impedance of the media, (3) media attenuation, (4) transmission frequency, and (5) attached electric loads. The authors describe a solution to prevent the standing wave by using frequency sweeps (rang of frequency operation) with wave bursts. Depend on the thickness of the wall a number of the burst cycle can be used, as an example five cycles for aluminum and ten cycles for POM. The results showed that the maximum power transfer efficiency occurs when there is a match impedance between the medium and the PZT.

Shi et al. [27] pointing out that the volume of the battery typically takes up 2/3 of the volume of medical implanted devices, such as a pacemaker. These batteries need to be replaced by a surgical procedure that exposes the patients to health risks. Two methods to avoid this surgical procedure are harvesting energy from the periodical vibration of the heart or lungs and using a piezoelectric device. The authors report that the acoustic power transfer method can transfer energy for more than 15 cm. In the absence of a matching layer, ultrasound is reflected back and forth between the two PZTs surfaces leading to a standing wave between the PZTs with peaks and valleys of power and transfer efficiency. Since the human body has different thicknesses, sometimes it will be difficult to avoid a minimum value of voltage due to standing wave effects. This problem can be

solved by continuously changing the frequency of operation because it can change the location of the peak and valleys. The authors suggest using microelectromechanical systems (MEMS) to extend the battery lifetime. One such system is the piezoelectric ultrasound energy harvester (PUEH) fabricated from the PZT diaphragm array (diaphragm array: consists of 7 PZT diaphragms that are connected in parallel).

The points of maxima voltage can be found by using the following equation:

$$D = n \times \frac{\lambda}{2} \tag{18}$$

$$\lambda = \frac{f}{c} \tag{19}$$

Where D is the distance between the transmitter and receiver, n is a positive integer. λ is the wave-length in medium, c is the speed of sound in medium (1480 m/s in water) and f is frequency. Changing the frequency will change the locations of maxima voltage points according to equations (18) and (19). The acoustic pressure can be measured by a hydrophone placed at one cm distance from the transmitter PZT. The intensity can be calculated by the following equation: $I = \frac{p^2}{2z}$, where I is the ultrasound intensity, p is the ultrasound pressure and Z is the acoustic impedance (for water medium, Z is 1.48×10^6 kg/m^2·s).

2.7 Acoustic Energy Transfer

Roes et al. [16] found that when low frequencies are used to transfer energy, the losses of acoustic energy transfer are also low. If the skin-depth is large, the low coupling between the transmitter and receiver means a large current is required, which results in high induction losses. Normally, large currents cause high induction losses, for that the fabrication company always gives the

frequencies range of operation. The range of frequencies for most of the applications is between (0.5 - 2.25 MHz).

The experimental paper of Roes et al. [16] showed a large reflection between TX and RX transducers, which caused maxima and minima as a function distance between the traducers. A sound source of the finite dimension will experience diffraction when the wave hits the receiver PZT, which leads to scatter that will reduce the efficiency of acoustic energy transfer.

Yan et al. [17] studied the parameters that affect the power transmitted to an implanted device in the far-field region. The implanted system was built and tested experimentally to analyze energy transmission. The authors discuss the effect of PZT skin depth, sound source frequency, and sound source excitation on energy propagation. They present the sound intensity as a function for distance, which decreases with increasing the distance. This means that there is a sound field that has directivity in the progress of propagation. As the frequency increase, the sound intensity decays faster.

Sometimes, normalization is needed to compare the simulation and experiment, A commonly used normalized formula is

$$x^* = \frac{x - x_{min}}{x_{max} - x_{min}} \tag{20}$$

where x_{min} and x_{max} are the minimum and maximum values in the data to be normalized. Yang et al. [18] studied the ultrasonic power transmission between transmitter and receiver where the medium between the two PZTs is an elastic wall. The results showed that the effective way to operate the device is at its resonant frequencies.

Rose et al. [20] worked to overcome the difficulties of energy transfer through the air using ultrasound. This study suggests a model that shows improvement in energy transfer that reached 53%. The experiment to validate the calculation showed 16% due to the low capability of the applied transducer. There are other reasons for losing the energy due to acoustic reflection between the transducers and the mismatch with the water impedance.

Lee et al. [21] designed a PZT system to power the brain-machine interface system. The resonance frequency of the PZT transmitter and receiver was 250 kHz. The maximum power transfer efficiency that the researcher reached was 55 % at a 1 mm distance and 243 kHz, while the old efficiency was 50% at 20 mm.

Shmilovitz et al. [22] fabricated an ultrasound energy transfer system using two piezoelectric transducers of equal size (15 mm × 3 mm) and operated at 720 kHz. The amount of energy transferred to the PZT receiver can't be predicted due to the following factors: (1) geometrical spread of the pressure wave (2) accumulated power loss in the tissue. (3) the relative physical orientation of the implanted receiver. The authors calculate the efficiency as the ratio of power received by the implanted transducer to the power consumed by the transmitting transducer. Moreover, the power required for the implanted PZT was not constant; thus, regulation of the amount of energy stored in the implant was required.

2.8 References

1. Tsui, C. Y., Li, X., & Ki, W. H. (2013). Energy harvesting and power delivery for implantable medical devices. Foundations and Trends® in Electronic Design Automation, 7(3), 179-246.

2. Basaeri, H., Christensen, D. B., & Roundy, S. (2016). A review of acoustic power transfer for bio-medical implants. Smart Materials and Structures, 25(12), 123001.

3. Mo, C., Hudson, S., & Radziemski, L. J. (2013, April). Effect of misalignment between ultrasound piezoelectric transducers on transcutaneous energy transfer. In Active and Passive Smart Structures and Integrated Systems 2013 (Vol. 8688, p. 868814). International Society for Optics and Photonics.

4. Christensen, D. B., Basaeri, H., & Roundy, S. (2017). A computationally efficient technique to model depth, orientation and alignment via ray tracing in acoustic power transfer systems. Smart Materials and Structures, 26(12), 125020.

5. Ozeri, S., & Shmilovitz, D. (2010). Ultrasonic transcutaneous energy transfer for powering implanted devices. Ultrasonics, 50(6), 556-566.

6. Rathod, V. T. (2019). A Review of Electric Impedance Matching Techniques for Piezoelectric Sensors, Actuators and Transducers. Electronics, 8(2), 169.

7. Ozeri, S., Shmilovitz, D., Singer, S., & Wang, C. C. (2010). Ultrasonic transcutaneous energy transfer using a continuous wave 650 kHz Gaussian shaded transmitter. Ultrasonics, 50(7), 666-674.

8. Gorostiaga, M., Wapler, M. C., & Wallrabe, U. (2017). Analytic model for ultrasound energy receivers and their optimal electric loads II: Experimental validation. Smart Materials and Structures, 26(10), 105021.

9. Lee, S. Q., Youm, W., & Hwang, G. (2013, June). Biocompatible wireless power transferring based on ultrasonic resonance devices. In Proceedings of Meetings on Acoustics ICA2013 (Vol. 19, No. 1, p. 030030). Acoustical Society of America.

10. Saat, S., Mokhtar, N. F., Zaid, T., Ghani, Z. A., Isa, A. A. M., Darsono, A. M., ... & Zin, M. S. I. M. (2015). The Development of Wireless Power Transfer Technologies for Low Power Applications: An Acoustic Based Approach. Journal of Telecommunication, Electronic and Computer Engineering (JTEC), 7(2), 129-135.

11. COMSOL Multiphysics® v. 5.4. www.comsol.com. COMSOL AB, Stockholm, Sweden

12. Shaul, O., Boaz, S., & Doron, S. (2012, May). Non-invasive sensing of the electrical energy harvested by medical implants powered by an ultrasonic transcutaneous energy transfer link. In 2012 IEEE International Symposium on Industrial Electronics (pp. 1153-1157). IEEE.

13. Silveira, E. S., Nascimento, D. C., & Pina, M. V. (2017). Design of Microstrip Antenna Array with Suppressed Back Lobe. Journal of Microwaves, Optoelectronics and Electromagnetic Applications, 16(2), 460-470.

14. Maleki, T., Cao, N., Song, S. H., Kao, C., Ko, S. C., & Ziaie, B. (2011). An ultrasonically powered implantable micro-oxygen generator (IMOG). IEEE transactions on Biomedical Engineering, 58(11), 3104-3111.

15. Agarwal, K., Jegadeesan, R., Guo, Y. X., & Thakor, N. V. (2017). Wireless power transfer strategies for implantable bioelectronics. IEEE reviews in biomedical engineering, 10, 136-161.

16. Roes, M. G., Duarte, J. L., Hendrix, M. A., & Lomonova, E. A. (2012). Acoustic energy transfer: A review. IEEE Transactions on Industrial Electronics, 60(1), 242-248.

17. Yan, X., Zhu, Z., Liu, G. Q., & Zhao, X. (2019). Analysis of Implantable Ultrasonic Coupling Wireless Power Transmission System. Progress In Electromagnetics Research, 80, 203-214.

18. Yang, Z., Zeng, D., Zhao, C., Li, F., & Wang, H. (2013, October). Wireless energy transmission using ultrasound for implantable devices. In 2013 Symposium on Piezoelectricity, Acoustic Waves, and Device Applications (pp. 1-4). IEEE.

19. Awal, M. R., Jusoh, M., Sabapathy, T., Kamarudin, M. R., & Rahim, R. A. (2016). State-of-the-art developments of acoustic energy transfer. International Journal of Antennas and Propagation, 2016.

20. Roes, M. G. L., Hendrix, M. A. M., & Duarte, J. L. (2011, November). Contactless energy transfer through air by means of ultrasound. In IECON 2011-37th Annual Conference of the IEEE Industrial Electronics Society (pp. 1238-1243). IEEE.

21. Lee, S. Q., Youm, W., Hwang, G., Moon, K. S., & Ozturk, Y. (2014, March). Resonant ultrasonic wireless power transmission for bio-implants. In Active and Passive Smart Structures and Integrated Systems 2014 (Vol. 9057, p. 90570J). International Society for Optics and Photonics.

22. Shmilovitz, D., Ozeri, S., Wang, C. C., & Spivak, B. (2013). Noninvasive control of the power transferred to an implanted device by an ultrasonic transcutaneous energy transfer link. IEEE Transactions on Biomedical Engineering, 61(4), 995-1004.

23. Salani, M., Roy, S., & Fissell IV, W. H. (2018). Innovations in wearable and implantable artificial kidneys. American Journal of Kidney Diseases, 72(5), 745-751.

24. Mahmood, M. F., Mohammed, S. L., & Gharghan, S. K. (2019). Ultrasound sensor-based wireless power transfer for low-power medical devices. Journal of Low Power Electronics and Applications, 9(3), 20.

25. Zaid, T., Saat, S., Jamal, N., Yusop, Y., Huzaimah H, S., & Hindustan, I. (2016). A Study on Performance of the Acoustic Energy Transfer System Through Air Medium Using Ceramic Disk Ultrasonic Transducer. JApSc, 16(12), 580-587.

26. Kar, B., & Wallrabe, U. (2020). Performance Enhancement of an Ultrasonic Power Transfer System Through a Tightly Coupled Solid Media Using a KLM Model. Micromachines, 11(4), 355.

27. Shi, Q., Wang, T., & Lee, C. (2016). MEMS based broadband piezoelectric ultrasonic energy harvester (PUEH) for enabling self-powered implantable biomedical devices. Scientific reports, 6, 24946.

CHAPTER THREE: Methodology

3.1 Introduction

In this chapter, a finite element method (FEM) for a medical implantable device is developed to set the variables and the boundary conditions for getting simulated results. This chapter discusses the theoretical and experimental method used to investigate the sending receiving ultrasound signal. The FEM is used to predict the power transfer from the PZT-transmitter to the PZT-receiver.

3.2 Ultrasound power transfer system using PZT-5H

The ultrasound power transfer system using PZT-5H was simulated using COMSOL software [1]. The stimulation frequency was 1 MHz except in those cases where the effects of frequency were investigated. To maximize the powering efficiency, it is important to match both the resonant frequency of PZT and the acoustic impedance of soft tissue. The properties of the PZT-5H used in the experimental validation of simulation results are listed in Table 2.

Table 2: PZT-5H properties [1].

Density	7500 kg/m^3
Speed of sound	2012.5 m/s
Thickness	1.9 mm
Diameter	12.7 mm
Mechanical quality factor	80

In this dissertation, the simulation of both piezoelectric transducers can have offset, depth, and angle within the defined coordinate system. The receiver rotation angle is defined as misalignment between the PZT transmitter and receiver. The PZT rotation angle was varied to investigate the

effect of the misalignment of the transducers on the output voltage. Simulations were done for the distance between the transmitter and receiver varied between 5 and 16 mm and rotation angle varied between 0 to 5 degrees. Due to the difficulties of using tissue samples in experiments to validate model prediction, water was used as the medium in both calculations and experiments. Nevertheless, to emphasize the importance of our work for medical implanted devices, we will refer to the distance between transmitter and receiver as “skin depth”.

A piezoelectric energy transfer system consisting of two PZT-5H transducers is analyzed in this work because it has mechanical properties close to those of the PZT used by Christensen et al. [4] for their analysis and experimental validation. This will make it easier to compare our results and apply the same boundary condition to validate the results.

3.3 Experimental Validation

Figure 4 illustrates an experimental apparatus constructed to validate the simulation results. PZT-5H was fitted inside a 0.5-inch metal pipe. Advanced Silicone (General Electric Company) was used to fix the PZT transducers inside the pipe and to serve as an isolation layer between the PZT and the galvanized pipe. This galvanized pipe will be changed later to PVC to insure more isolation.

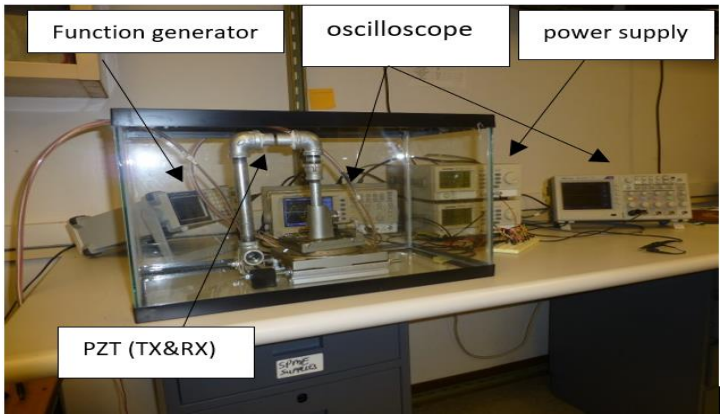

Figure 4: Experimental setup.

The PZT transmitter was connected to an angular and axial micrometer then submerged in water, as shown in figure 5. The waterproof wires were connected to the PZT transducers then to the amplifier circuit. The circuit is connected to a function generator as well as a DC voltage power supply. The measured output voltages were compared with the simulation results.

To verify the performance of the system, measurements of ultrasound radiation and energy transfer were conducted inside a homemade water tank, using water at room temperature (25°C). Distilled water was used as the medium for acoustic wave propagation since its acoustic impedance is close to that of soft biological tissue. The transmitter and receiver are inserted in the water bath facing each other.

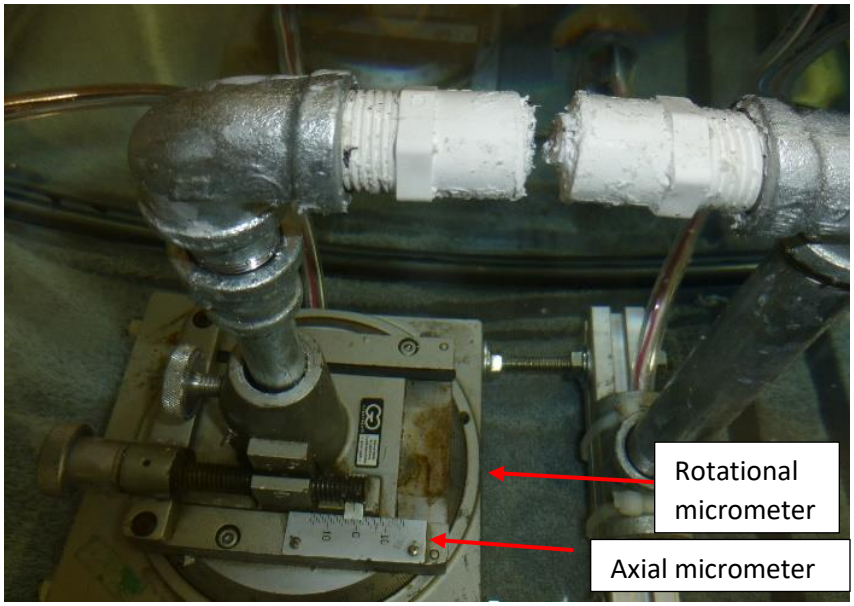

Figure 5: Axial and rotational micrometers inside the aquarium.

3.4 Ultrasound power transfer system using modified PZT-4

The ultrasound power transfer system using modified PZT-4 was simulated using COMSOL software [1]. To maximize the power-transfer efficiency, it is important to match both the resonant

frequency of PZT and the acoustic impedance of soft tissue. The properties of the PZT-4 used in the experimental validation of simulation results are listed in Table 3.

Table 3: Modify PZT-4 properties [2].

Density	7900 kg/m^3
Speed of sound for thickness vibration mode (Nt)	2070 m/s
Thickness	2.07 mm
Diameter	21 mm
Speed of sound for PZT (Np)	2200 m/s
Mechanical quality factor	1800

Mechanical quality factor is the ratio of the initial energy stored in the resonator to the energy lost in one radian of the cycle of oscillation as in the following equation [3].

$$\text{Mechanical quality factor} = \frac{Energy\ stored}{Energy\ loss} \tag{21}$$

3.5 Theoretical formulation

The COMSOL 5.5 software tree window was built by using the four major domains: Pressure acoustic that contains the frequency domain, Solid Mechanics, Electrostatic equation, and Electric circuits.

1. Pressure Acoustics, Frequency Domain equation

$$\nabla \cdot \left(\frac{-1}{\rho_0}(\nabla p - q)\right) - \frac{\omega^2 p}{\rho_0 c^2} = 0 \tag{22}$$

Where ρ_0 is the density of the fluid, c = speed of sound, p = pressure, q= dipole source, and $\omega = 2\pi f$.

2. Solid Mechanics equation

$$\nabla \cdot (Fs) + (F_v) = -\rho\omega^2 u \quad (23)$$

Where s = stress, ρ = density, u = displacement, F = gradient deformation, ω = angular velocity, and F_v= body force per unit deformed volume.

3. Electrostatic equation = Maxwell equations

$$\nabla \cdot E = \rho, \text{ E = electric field} \quad (24)$$

$$\nabla \cdot \text{B} = 0, \text{ B = magnetic filed} \quad (25)$$

3.6 COMSOL model builder

The software model builder consists of four major parts: pressure acoustic, frequency domain, solid mechanics, electrostatic and electric circuit, as shown in figure 6. The pressure applied to the system was the continuous wave transfer. A Solid mechanics was applied to the PZT material. Electrostatic was applied to the whole systems (water and PZT). The electric circuit builder was used to connect the PZT-transmitter to the electric power supply and the PZT receiver to the load resistor.

Figure 6: COMSOL software model window.

3.7 References

1. COMSOL Multiphysics® v. 5.4. www.comsol.com. COMSOL AB, Stockholm, Sweden
2. https://www.steminc.com/piezo/PZ_property1.asp
3. https://en.wikipedia.org/wiki/Q_factor

CHAPTER FOUR: Simulating ultrasound power transfer system using PZT-5H in the near field and experimental validation

4.1 Simulation model validation

Figure 7 shows simulation results from the PZT model built in COMSOL software as described in the previous chapter. The PZT diameters for the transmitter and receiver are identical (12.7 mm). The dots connected by blue lines are the simulated results. The red circles in the figure are measured voltage output at different separations of TX and RX determined by the micrometer attached to the transmitter. It is noted that the measured values are lower than the calculated values by essentially the same amount throughout the range of measurement. This systematic difference between simulation and experimental data is probably due to the fact that our simulations do not precisely reproduce the experimental setup. For example, they do not include the wires connecting TX and RX to measurement devices. Other than this small constant difference in magnitude the agreement between simulations and experimental data is good.

The magnitude of the voltage applied at the TX is ±16 V. Between 12.5 to 16 mm, the pattern of oscillation predicts by COMSOL software is similar to that calculated by Christensen et al. [1] for the same distance. PZT-5H has a mechanical quality equals of 65, which makes it similar to the one used in [1] with a Q equal to 80. The similarity between the results predicted by different computation methods gives us more confidence in our use of the COMSOL software package.

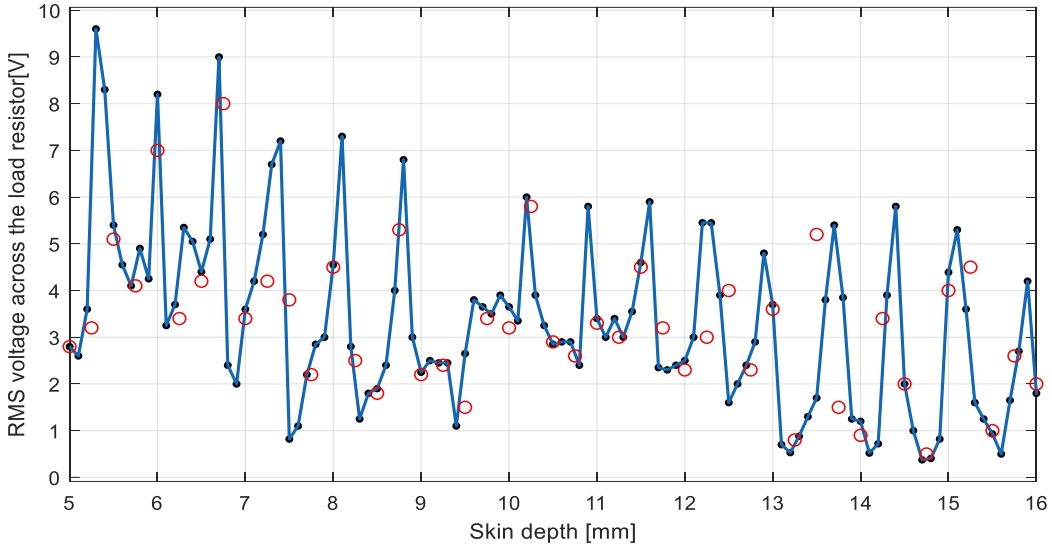

Figure 7: Output voltage at the receiver versus skin depth. The red circle refers to the experimental measurement validation.

Figure 7 shows the simulated and measured voltage output with respect to skin depth (a term used by COMSOL software to indicate the distance between TX and RX, center to center). The PZT transmitter was moved backward by using a micrometer to change the skin depth. The measurements were taken from a distance of 5 mm to 16 mm, with increments equal to 0.25 mm. The red circle represents the measured results, while the solid line is the simulation results. The result showed a good match between the theoretical and experimental. In our case, the range fo the near field for TX is given by $L = \frac{a^2}{wavelength} = \frac{(0.0127/2)^2}{\frac{1730}{1058824}} = 24.7\ mm$, where 1730 is the speed of sound inside the skin, which means that the results in Figure 7 apply to the near field (NF) only.

4.2 Acoustic pressure

Figure 8 shows how the maximum RMS acoustic pressure changes with skin depth. The maximum pressure peak appeared at a depth of 5.3 mm. We will use this distance between TX and RX to understand the effect of this maximum pressure on optimization. At depths between 5 mm to 16

mm, the results show sinusoidal variation while the envelope of the signal decreases due to absorption of the ultrasound wave [3].

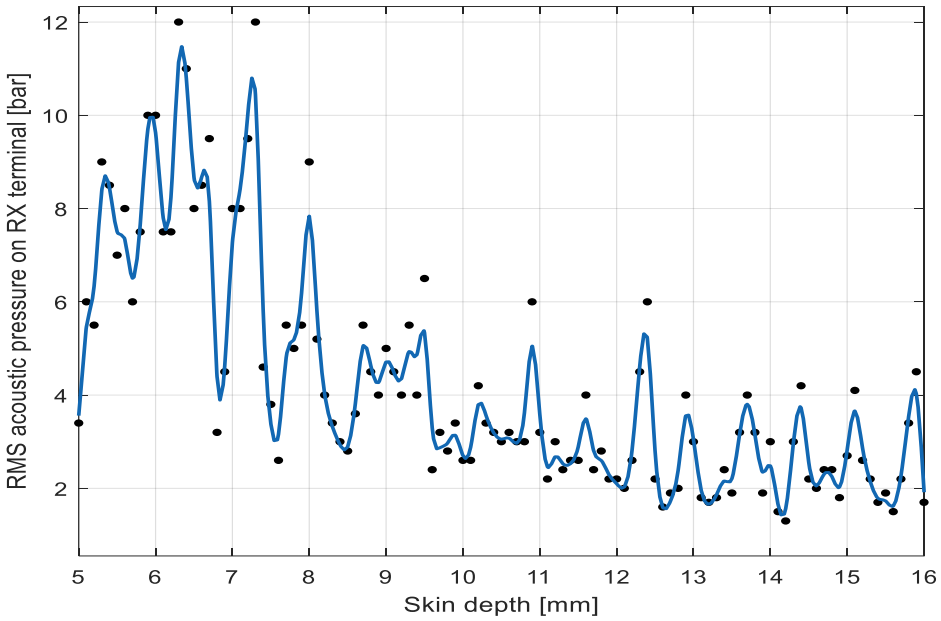

Figure 8: The acoustic pressure with respect to skin depth.

The boundary between two materials of different acoustic impedances is called an acoustic interface. When sound strikes an acoustic interface at normal incidence, some amount of sound energy is reflected, and some amount is transmitted across the boundary. The dB loss of energy on transmitting a signal from medium 1 into medium 2 is given by [4]

$$dB\ \ loss = 10\log_{10}[4 \times Z_1 \times \frac{Z_2}{(Z_1 \times Z_2)^2}] \tag{26}$$

z_1, z_2 are acoustic impedances for the first and second material, respectively.

4.3 Misalignment

Figure 9 shows how the power transfer efficiency on the receiver PZT changes with various skin depth and misalignment. The 3D plot in Figure 9 shows how power transfer efficiency on the receiver PZT changes with various combinations of skin depth and misalignment. For a given amount of misalignment, output efficiency oscillates with changing distance between transmitter and receiver. This behavior is particularly pronounced for small amounts of misalignment of the order of 1-2 degrees. The frequency used in these calculations is 1 MHz. It was found that increasing this misalignment as well as the skin depth can decrease the power transfer efficiency.

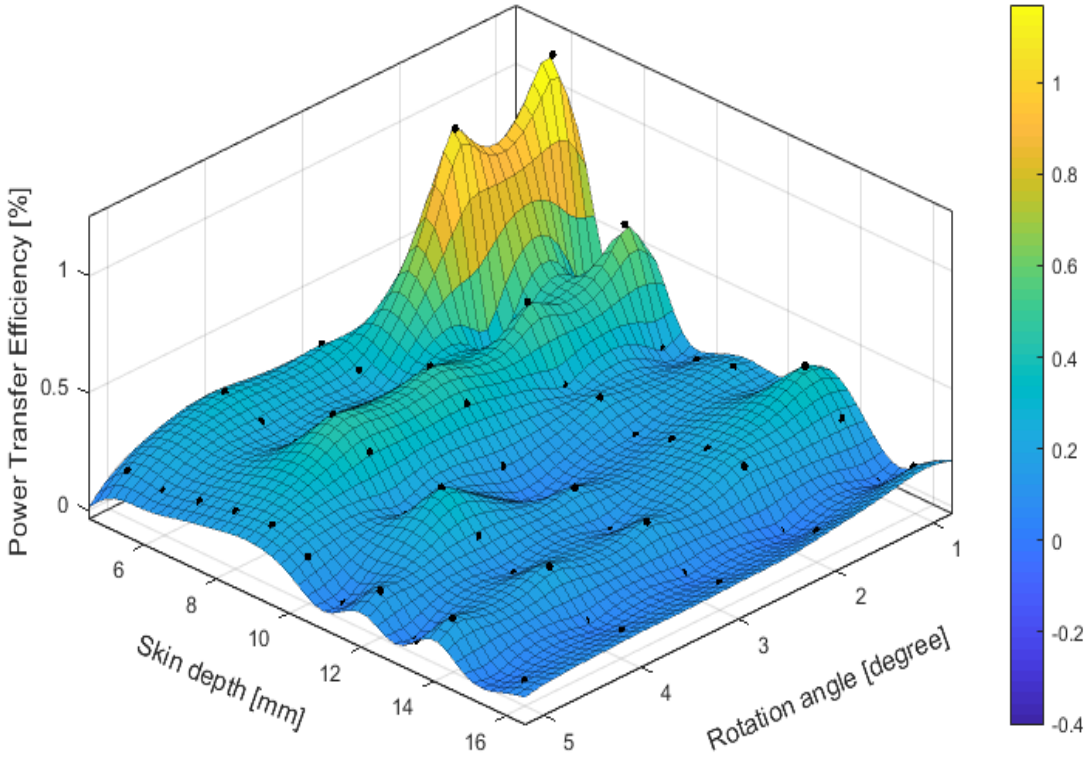

Figure 9: PZT Rotation angle, skin depth versus voltage.

The dots in Figure 10 show theoretical simulation results. The small red circle represents the experimental validation results. The distance between the PZT transmitter and receiver is 16 mm. The experimental setup does not allow the investigation of large angles of misalignment at small skin depths because the transmitter and receiver will touch. Figure 10 shows the agreement between theory and experiment over a wide range of misalignment when the separation between TX and RX is 16 mm. The blue curve is a spline fit to simulation results.As in Figure 7, experimental results have a small systematic difference from simulation results; nevertheless, the overall agreement is good. The agreement between theory and experiment at 0 and 5 degrees is partial validation of the complex relationship between skin depth and misalignment shown in Figure 9.

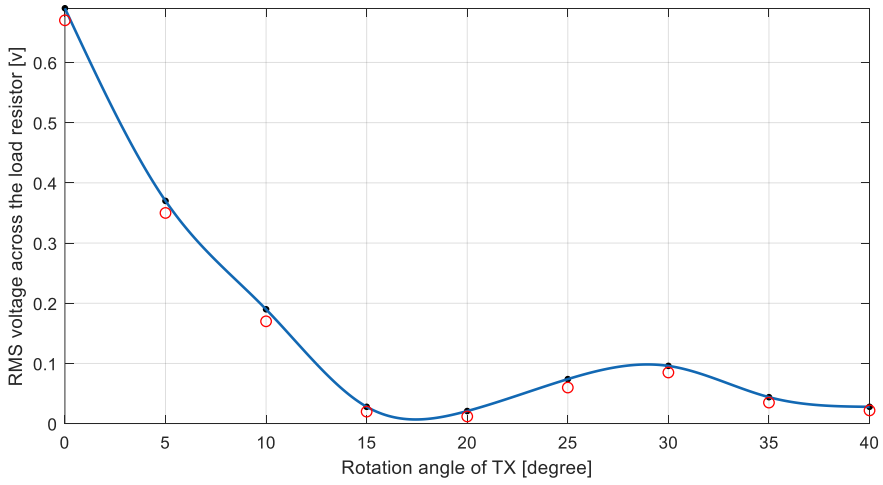

Figure 10: RMS voltage output versus rotation angle of TX.

4.4 Thickness, diameter, and radiation pattern

One advantage of simulation is that it can investigate effects that are not easily explored experimentally. Results of this type are shown in Figure 11 where effects on the power transfer efficiencies of the varying receiver and transmitter thickness have been calculated. The RX and

TX diameter is 12.7 mm and the separation of RX and TX is 6.3 mm. A peak in power transfer efficiency is calculated at RX thickness of 2 mm and TX of 2.25 mm thickness.

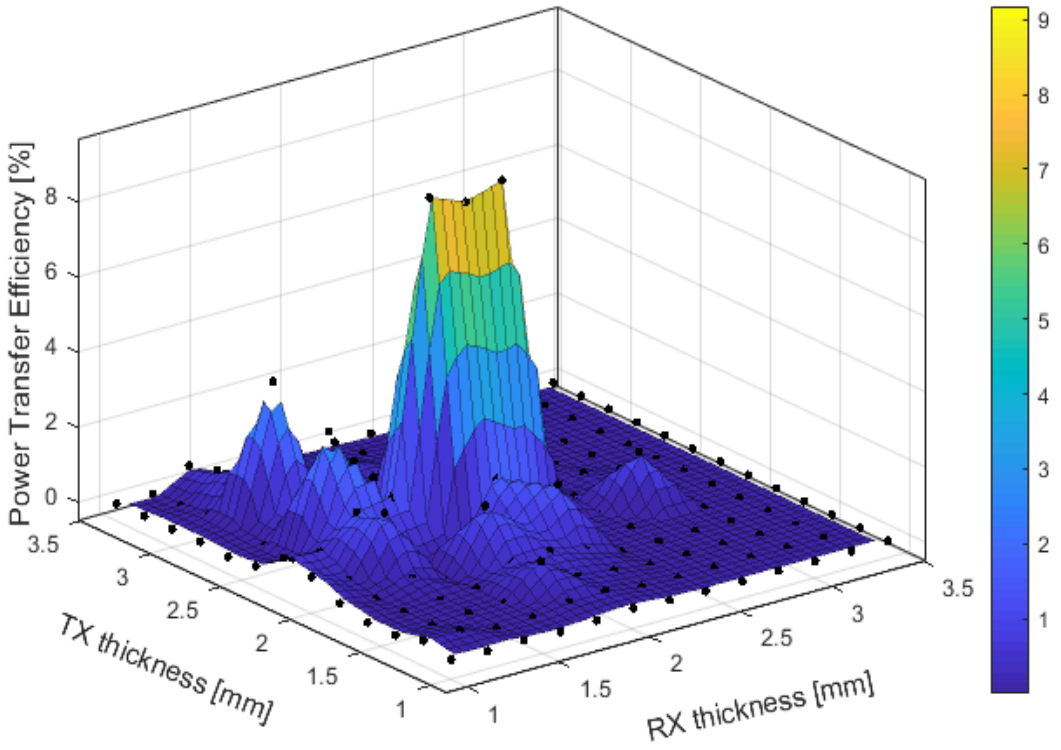

Figure11: RX and TX thickness versus output voltage

Figure 12 shows simulation results for the effect on the power transfer efficiency of changes in excitation frequency and skin depth. For frequencies above 900 kHz, these results suggest that increasing frequency results in higher power transfer efficiency. A peak of 20% power transfer efficiency is predicted at a frequency of 1200 kHz for a skin depth of 5 mm. Multiple peaks of similar height are encountered as the skin depth increases to 16 mm. The absence of any high-power transfer efficiency peaks at frequencies below 900 kHz shows that the system has good power transfer efficiency only when the system is close to the fundamental frequency.

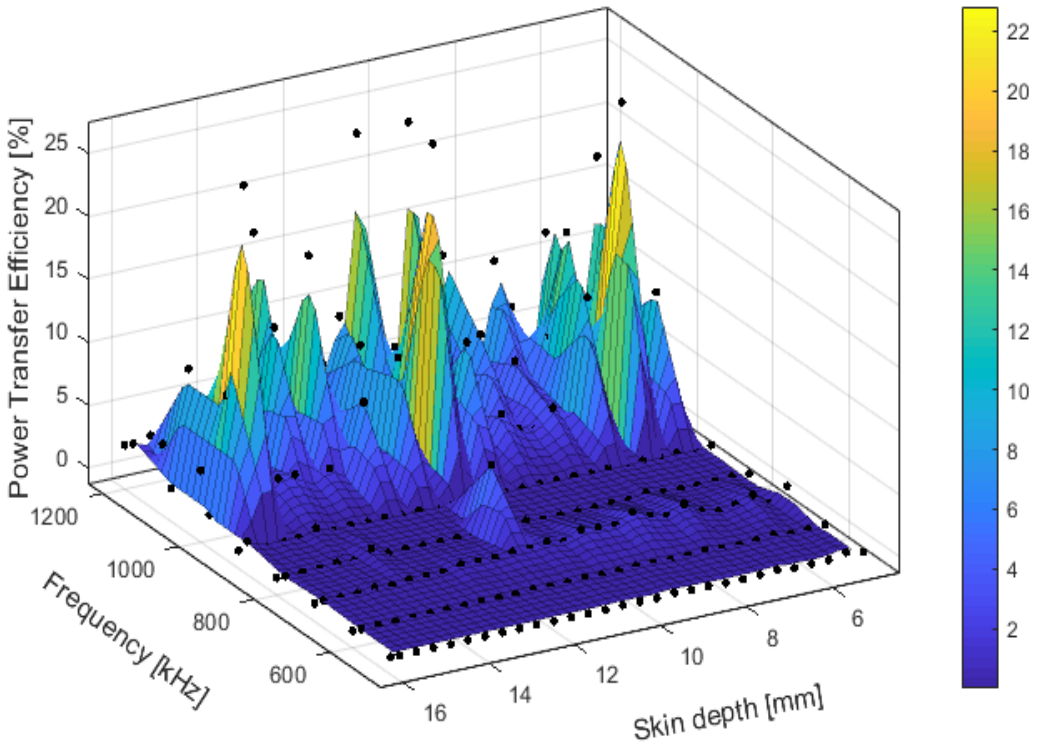

Figure 12: Frequency effect on the output voltage.

Figures 13 shows the calculated effects on power transfer efficiency obtained by the varying receiver and transmitter diameters. The thickness of RX and TX is 1.9 mm and their separation is 6.3 mm. Large transmitter diameter and small receiver diameters favor high power transfer efficiency. Increasing the transmitter diameter increases the area that generates the ultrasound wave. For a large transmitter diameter, increasing receiver diameter generates more reflected waves between the TR and RX. Figure 9 suggests this effect will decrease the power transfer efficiency.

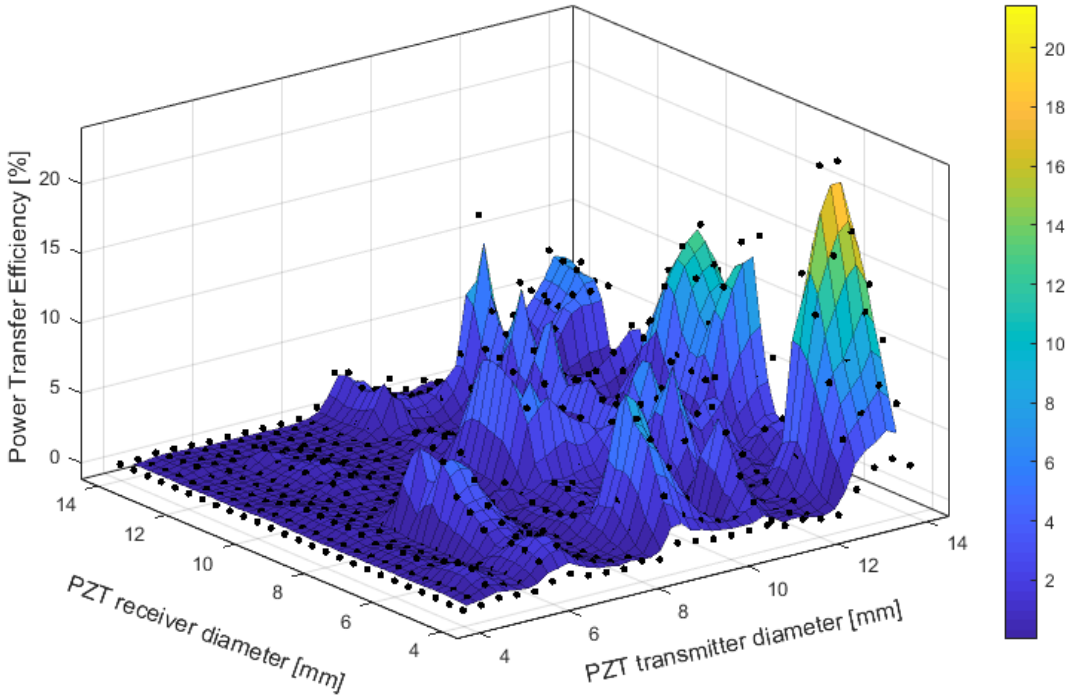

Figure 13: Effect of the PZT Transmitter and Receiver diameter on the voltage.

The acoustic pressure source was simulated by applying the electric voltage on the transmitter surface. From the 3D image in Figure 14, the acoustic pressure is shown to be a fluctuating wave. Each point on the PZT transmitter could be treated as an independent point source of radiation [2], in other words, the acoustic field is the vector sum of all these points. Two-dimensional and three-dimensional models generated the same results because the acoustic source can be considered as a point-shape, or a partial or total spherical surface around a point [5]. Each vibrating point on the transmitter surface could be considered as a point source emitting a spherical wave [6].

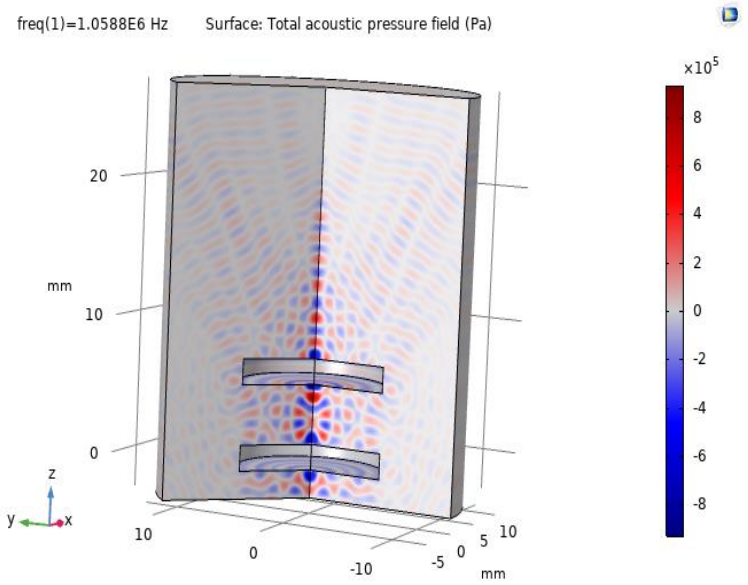

Figure 14: Total acoustic pressure field (Pa), 3D acoustic pressure (Pa).

The sound pressure field for this simulation is shown in figure 15. The sound that emanates from a piezoelectric transducer does not originate from a point but instead originates from most of the surface of the piezoelectric element. The intensity of the sound is indicated by color. The red indicates a higher intensity. Since the ultrasound originates from several points along the transducer face, the ultrasound intensity along the beam is affected by constructive and destructive wave interference [6], some points equal to zero while others equal to maximum.

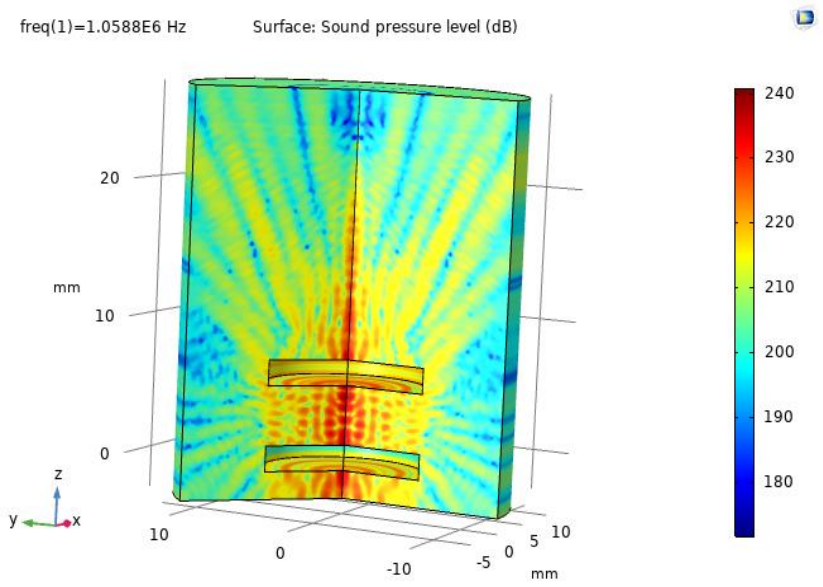

Figure 15: Three-dimensional sound pressure level (dB).

Figure 16 is a graphical representation of the radiation properties of the PZT transducer as a function of space [3]. The pattern describes how the transducer radiates energy into space. The main lobe is in the zero-degree direction. There are two main lobes perfectly mirrored as shown in figure 16. The pattern also shows the direction the PZT transducer needs to point to get a stronger signal. Elimination of the sidelobe and the back lobe is a must to improve the performance and save energy. The variation in sound pressure level between 0 and 90 degress is 150 dB. The gain is used to show how strong a signal could be generated from a received ultrasound wave by a PZT. Gain is the result of comparing power transmitted or received by PZT in a specific direction to the power received or transmitted by hypothetical ideal PZT in the same direction.

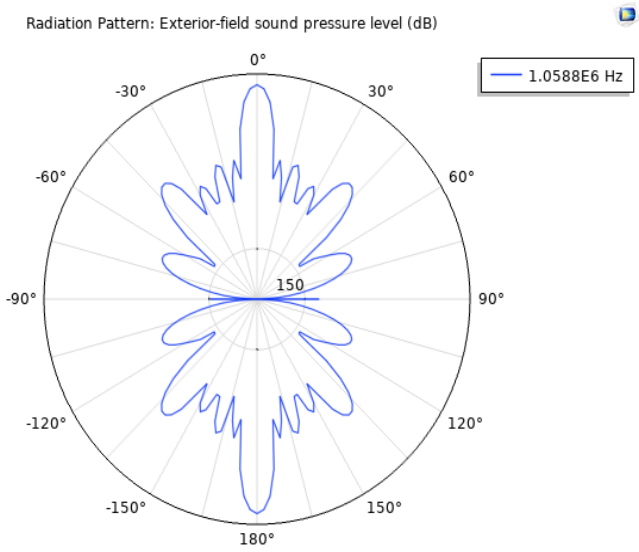

Figure 16: Radiation Pattern: Exterior-field sound pressure level (dB).

The PZT transducer with wide beam widths has a lower gain than that with narrow beamwidths. Note that the higher gain does not imply that the PZT transducer creates more power. It means that the same amount of power is radiated in a more focused way [7]. Figure 17 shows that the front-to-back ratio is equal to one. If the gain is increased, the number of side lobe generally goes up as well. When the PZT transmitter is close to the PZT receiver these side lobes can not affect the performance of the system [3]. Increasing the pressure field that consists of the main lobe causes the lower side lobe amplitudes to increase. Sidelobe that travels in parallel with the main lobe tends to decrease the amount of energy harvested by the PZT receiver [8].

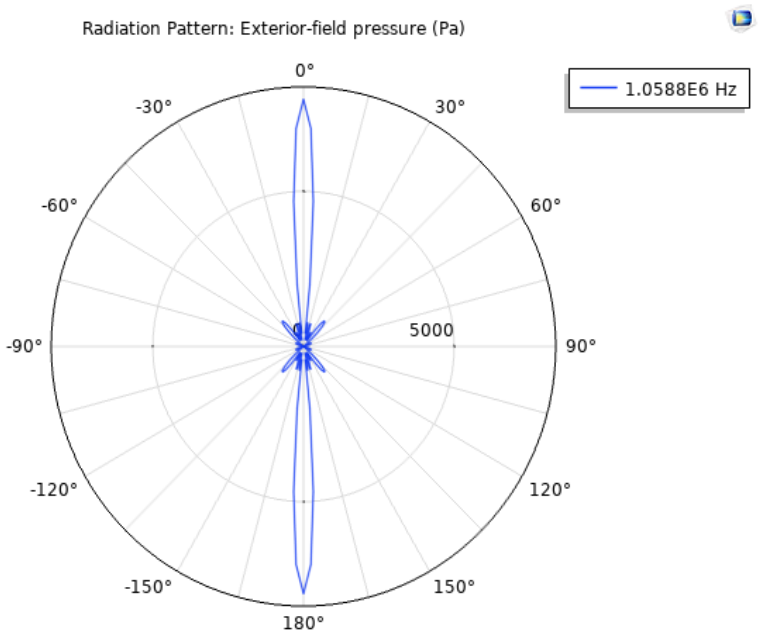

Figure 17: Radiation Pattern: Exterior-field pressure (Pa).

4.5 Thickness and diameter ratio, and misalignment

Figure 18 shows that the ratio of the diameter of the receiver to the diameter of the transmitter can affect the voltage generated from the system. When the TX= 1 mm and $\frac{RX}{TX}$ diameter ratio equal 2, the voltage generated is 12 volts on the PZT load resistance. When the transmitter diameter becomes smaller than that of the receiver, more energy will be captured by the receiver.

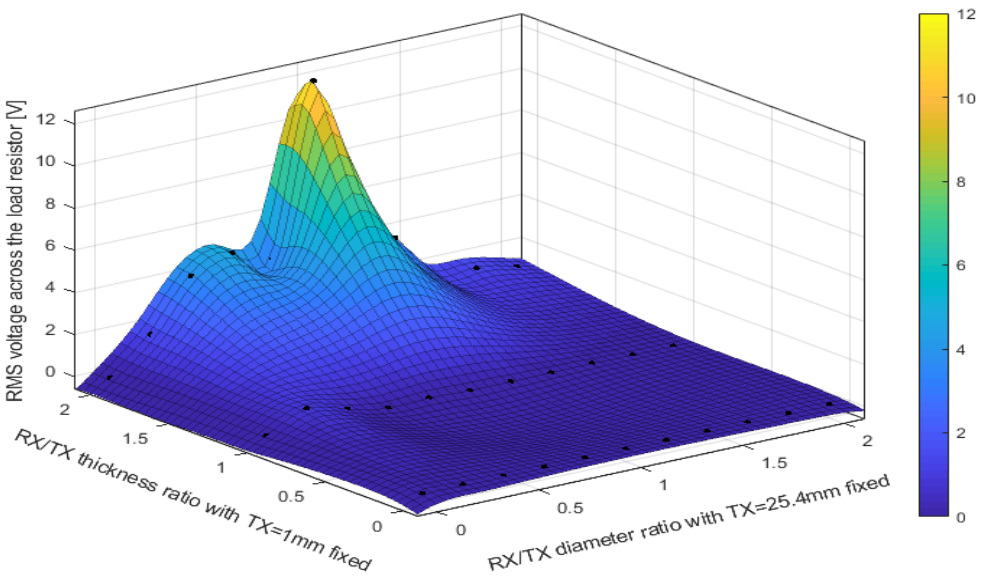

Figure 18: Thickness, diameter vs. voltage, with TX thickness= 1 mm.

Figure 19 investigates the simultaneous effect of the diameter ratio and thickness ratio on the voltage generated. At any diameter ratio, the highest voltage occurs at equal thickness. The ridge at equal thickness presents two peaks; a 10 V peak where diameter ratio is 0.5 and a 6 V peak where diameter ratio is 1.5.

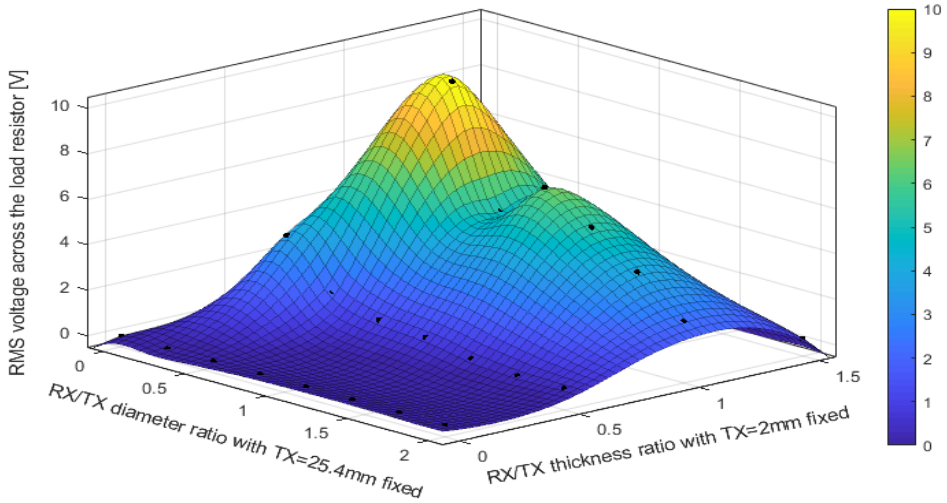

Figure 19: Thickness, diameter vs. voltage, with TX thickness = 2 mm.

In figure 20, the TX thickness equals 3mm, but the voltage generated is less than those shown in figures 18 and 19. This means that increase in the transmitter thickness doesn't mean that the voltage is increased but it means that we need to supply higher frequency to overcome acoustic impedance of the skin.

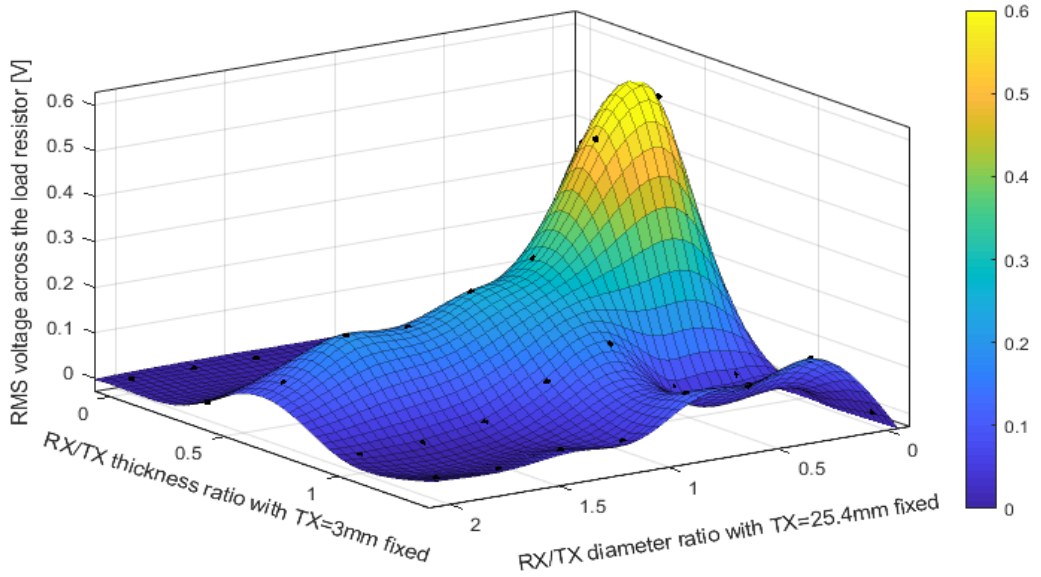

Figure 20: Thickness, diameter vs. voltage, with TX thickness= 3 mm.

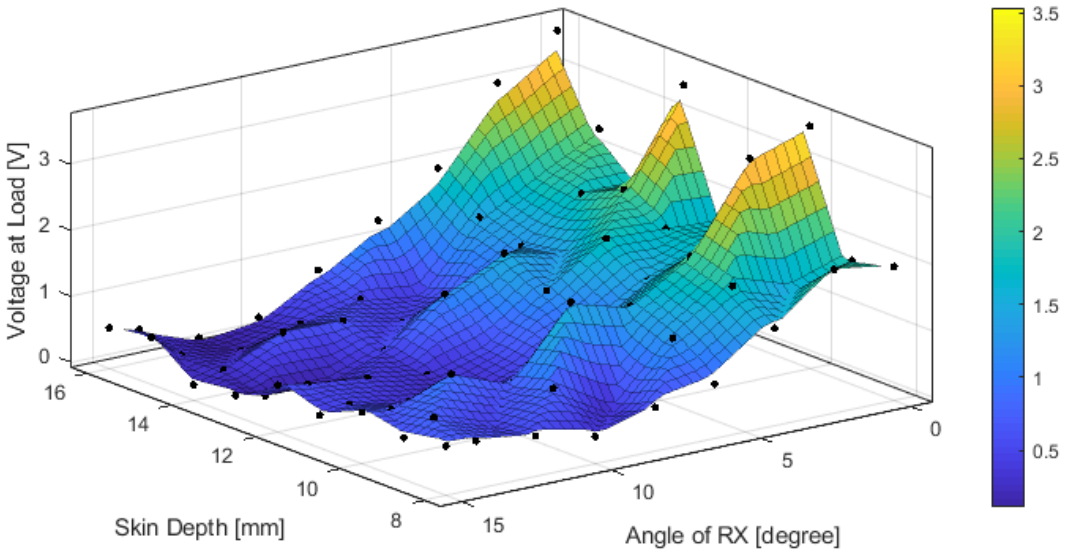

Figure 21: Skin depth vs. RX angle rotation as a function for voltage.

Figure 21 shows three peaks of the near field region when PZT receiver angles equal zero. Each peak has a ridge of decreasing voltage as the angle of rotation increases.

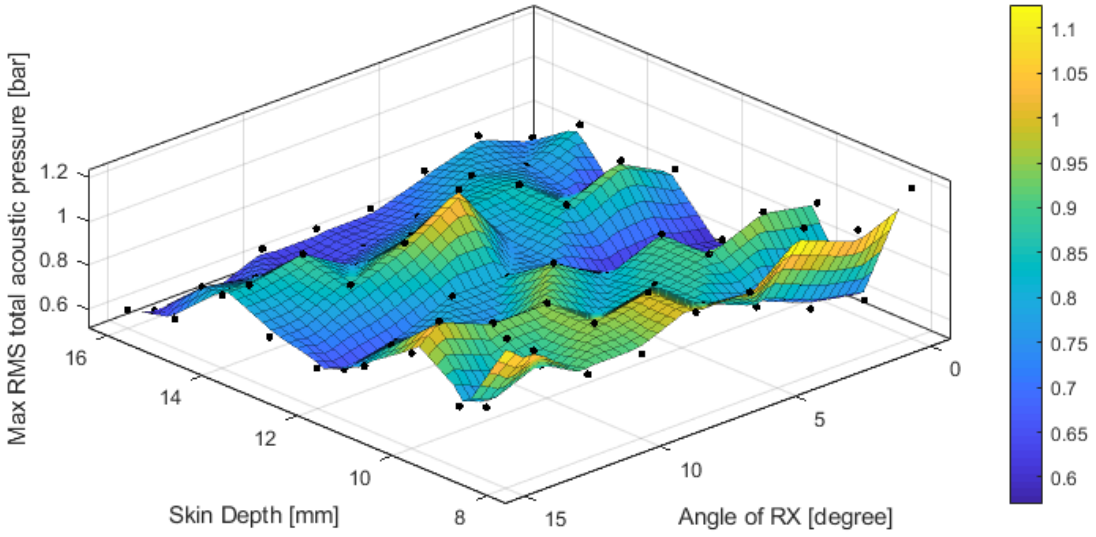

Figure 22: Skin depth vs. RX angle rotation, both as a function for RMS voltage.

Figure 22 shows that both the configuration of the PZT and the pressure acoustic contribute to the design of high-power system transfer. There is a peak of acoustic pressure where the skin-depth equals 13 mm and rotation angle equals 8 degrees. This peak is caused by the standing wave. The wave moves up and down only, doesn't apply pressure on the PZT face. This explains why Figure 21 does not show a peck of voltage at this configuration.

4.6 References

1. Christensen, D. B., Basaeri, H., & Roundy, S. (2017). A computationally efficient technique to model depth, orientation and alignment via ray tracing in acoustic power transfer systems. Smart Materials and Structures, 26(12), 125020.

2. Ozeri, S., & Shmilovitz, D. (2010). Ultrasonic transcutaneous energy transfer for powering implanted devices. Ultrasonics, 50(6), 556-566.

3. Maleki, T., Cao, N., Song, S. H., Kao, C., Ko, S. C., & Ziaie, B. (2011). An ultrasonically powered implantable micro-oxygen generator (IMOG). IEEE transactions on Biomedical Engineering, 58(11), 3104-3111.

4. Lee, S. Q., Youm, W., & Hwang, G. (2013, June). Biocompatible wireless power transferring based on ultrasonic resonance devices. In Proceedings of Meetings on Acoustics ICA2013 (Vol. 19, No. 1, p. 030030). Acoustical Society of America.

5. Roes, M. G., Duarte, J. L., Hendrix, M. A., & Lomonova, E. A. (2012). Acoustic energy transfer: A review. IEEE Transactions on Industrial Electronics, 60(1), 242-248.

6. Yan, X., Zhu, Z., Liu, G. Q., & Zhao, X. (2019). Analysis of Implantable Ultrasonic Coupling Wireless Power Transmission System. Progress In Electromagnetics Research, 80, 203-214.

7. Silveira, E. S., Nascimento, D. C., & Pina, M. V. (2017). Design of Microstrip Antenna Array with Suppressed Back Lobe. Journal of Microwaves, Optoelectronics and Electromagnetic Applications, 16(2), 460-470.

8. Ozeri, S., Shmilovitz, D., Singer, S., & Wang, C. C. (2010). Ultrasonic transcutaneous energy transfer using a continuous wave 650 kHz Gaussian shaded transmitter. Ultrasonics, 50(7), 666-674.

CHAPTER FIVE: Power transfer efficiency

5.1 Introduction

This chapter studies the voltage conversion between two modified PZT-4 transmitters and receivers (PZT-4 modified by STEMINC Company). The power transfer efficiency for the PZT system was investigated (where high efficiency is of great importance) to find the optimum boundary condition to obtain high performance for the system. The power transfer efficiency of such a system depends on the mechanical quality factor of the PZT (1800), density (7900), and the dielectric constant (1400) between the two PZTs. PZT-4 and PZT-8 (studied in chapter four) are hard piezoceramic materials used for welding, cutting, sonar, etc [1]. The electrical load is attached to the PZT receiver and represents the IMD which is equal to 210 or 110 ohms. All the measurement has been done in the near filed from 5 to 16 mm. The resonance frequency of the PZT is determined by its thickness and the speed of sound of the piezoelectric material (N_t). The finite element method implemented in COMSOL was used to simulate the full acoustic power transfer system in detail.

The simulation results were used to discover the effect of each parameter (depth, size, frequency, thickness, voltage, and alignment) on the transfer voltage. Experimental verification is presented in each possible case and these boundary conditions are conducted to be the same with COMSOL software boundary condition. The RX was placed in the near-field, which will cause the RX to have high fluctuations in voltage or intensity as a function of depth [2].

5.2 Experimental results and validation

The first parameter of interest is the depth. As the axial distance between the TX and RX changes, the voltage across the load resistor fluctuated as a result of acoustic waves, as in figure 23. The data shows that voltage generally decreases with an increase in depth. However, for a fixed medium, the voltage and power delivered to the electrical load are dependent on the following system parameters: load impedance (either 210 or 110 Ohms were used in this calculation), operating frequency (one megahertz), RX position relative to the TX (from 5 to 16 mm), and TX-RX diameter (either 21 or 10 mm).

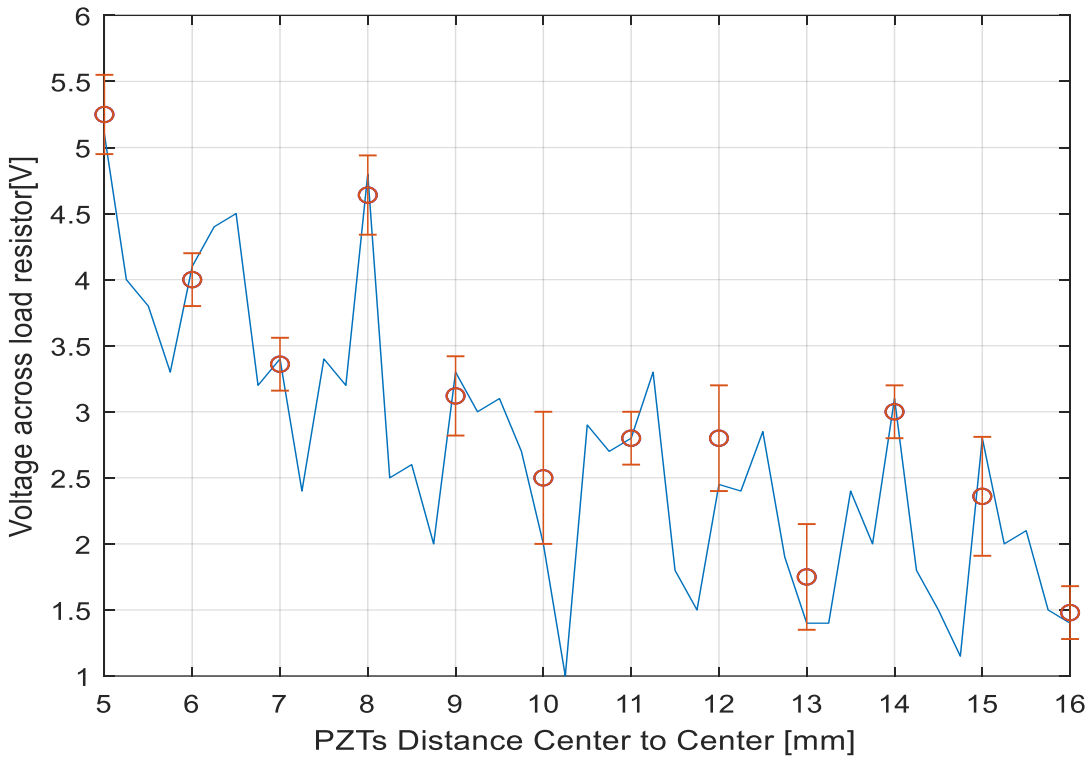

Figure 23: PZT diameter= 21 mm for RX & TX versus the voltage across the load resistor.The thickness of TX and RX equal 2.07 mm. The red circle represents the experimental results while the blue line represents the simulation results. The red vertical line represents the error bar.

Figure 24 shows simulation results have maximum efficiency at a 5 mm distance between TX and RX. The efficiency decreases when the distance increase until it reaches 1% at 16 mm.

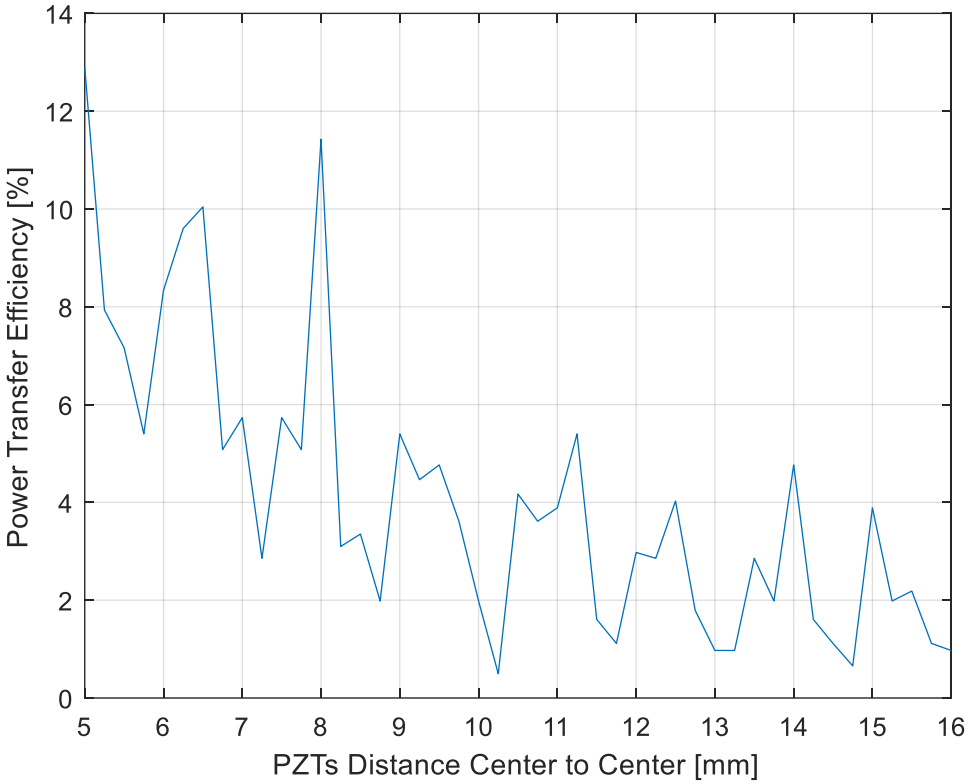

Figure 24 Power transfer efficiency as a function for the distance between the TX and RX when diameter= 21 mm for RX & TX.

The output voltage and experimental setup are presented in figure 25. The supply voltage Vpp (from the function generator) to the system is equal to 14.2 V. The measurement in figure 25 was done when the distance of TX to RX was equal to 5 mm. This resulted in a voltage equal to 10.2 V peak to peak or 5.1 V peak to zero, which is equal to 13.27% power transfer efficiency.

The output voltage peak-peak 10.2 V.

PZT TX and RX inside the aquarium.

Figure 25: Experimental setup when TX and RX have the same diameter of 21 mm.

Figure 26 shows the simulation results of TX and RX diameters of 21 and 10 mm, respectively. The highest voltage appears at 3.7 volts. This high voltage occurs when the distance between PZTs is 5 mm. The voltage fluctuats up and down at the same time it decreases, reaching 1.2 volts at a distance equal to 16 mm. At a distance of 6.5 mm, there is another high peak equal to 3.6 V.

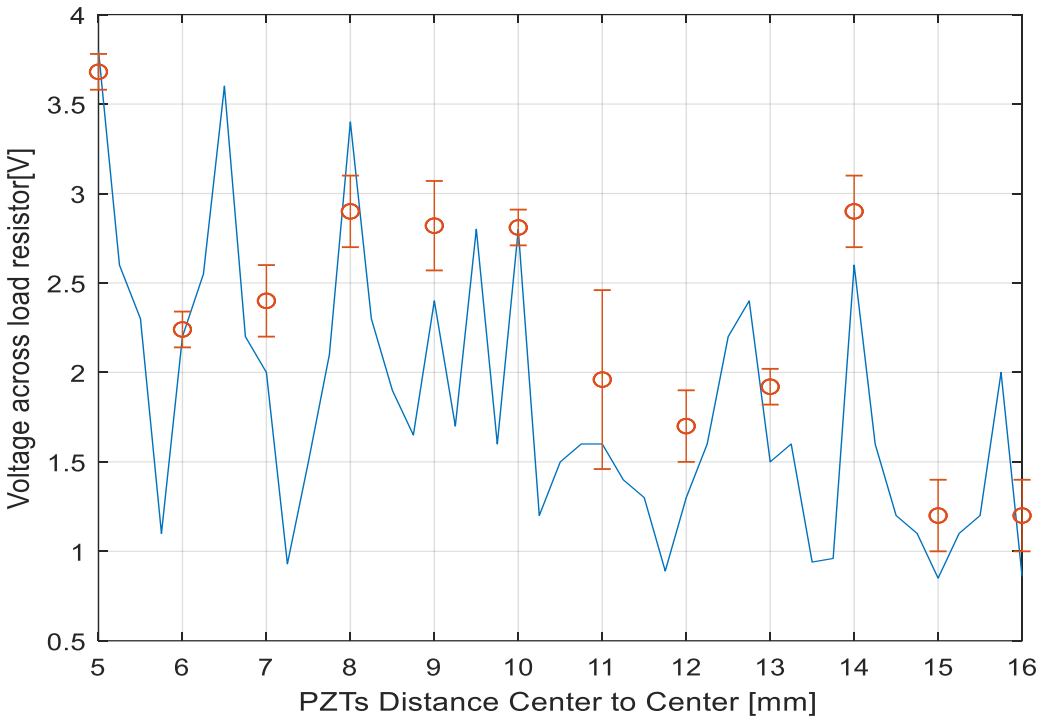

Figure 26: PZT-4 TX-diameter= 21 mm & RX-diameter= 10 mm. The thickness of TX and RX equal 2.07mm. The red circle represents the experimental results while the blue line represents the simulation results.

Figure 27 shows simuation results have maximum efficiency at a 5 mm distance between TX and RX. The efficiency decreases when the distance increases until it reaches 0.74% at a distance of 16 mm. Comparison of figures 24 and 27 indicate that a decrease in the size of the receiver from 21 mm to 10 mm can reduce the value of power transfer efficiency by half.

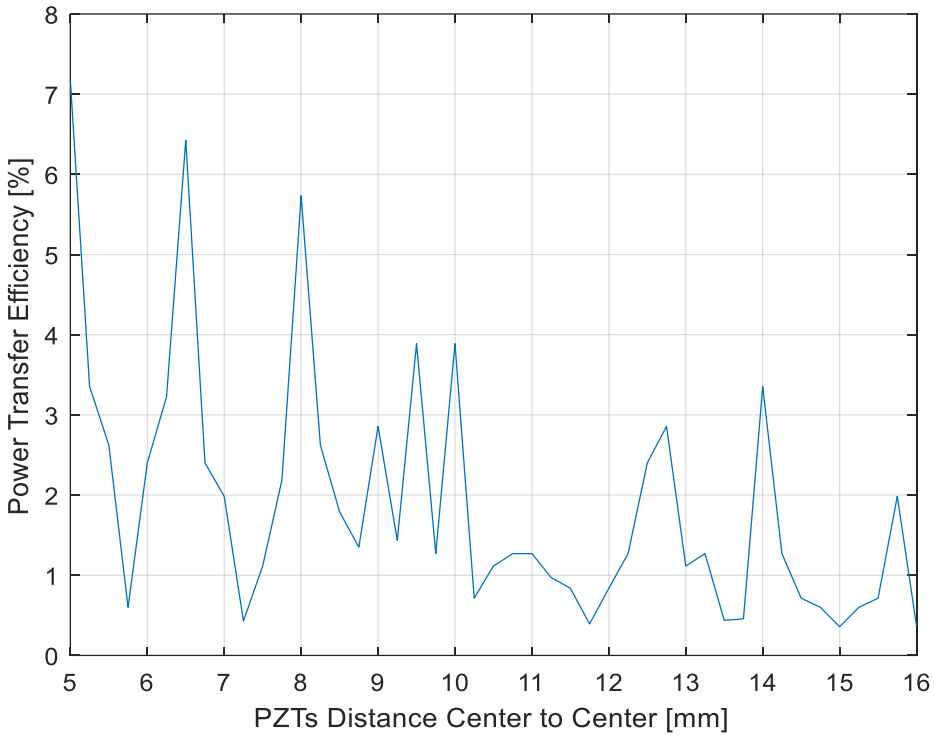

Figure 27: Power transfer efficiency as a function for the distance between the TX and RX, TX is bigger diameter than RX.

The voltage and the experimental setup are presented in figure 28. The Vpp represents the voltage peak to peak which is equal to 14.1 V. In this measurement the PZT's diameters are different but the material type is the same (modified PZT-4).

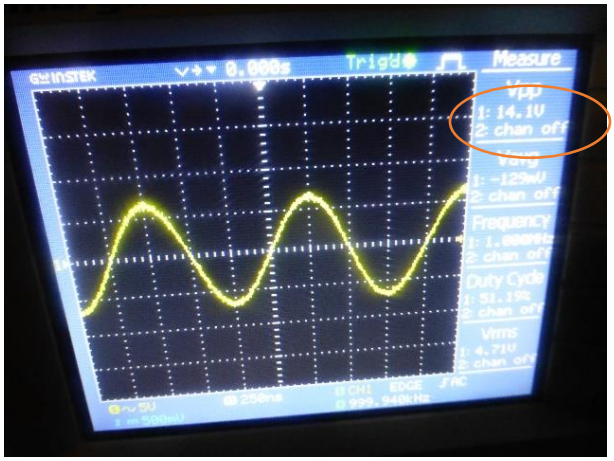

Oscilloscope measure the input voltage for TX.

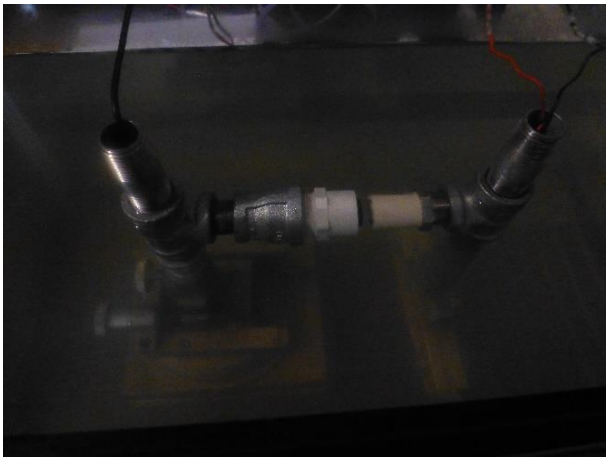

PZT TX and RX inside the aquarium.

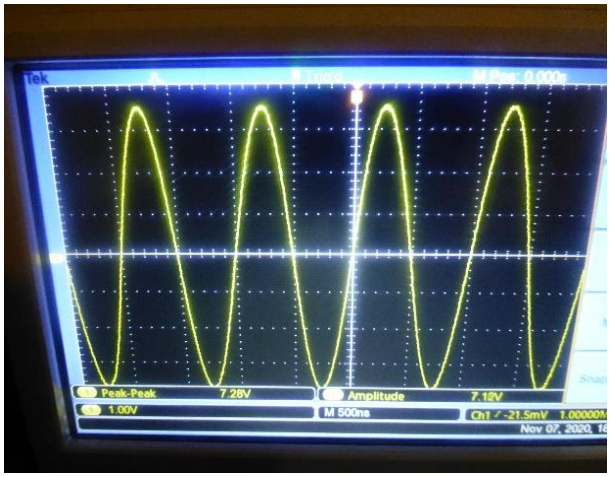

The output voltage peak-peak at 7.82 V.

Figure 28: Experimental setup when TX and RX have different diameter.

In figure 29 the PZT receiver has a bigger diameter (21 mm) than the PZT transmitter (10 mm). By comparing figure 26 to 29 it can be said that when the PZT receiver has a smaller diameter than the transmitter, a higher energy will be received by the RX. This may be related to the fewer reflections caused by the bigger RX diameter. The size of the implantable device is important in the design. Small implantable device size is preferred because when the size of the device increases, the required power also increases proportional to the surface area of the device. In that case, some of that energy would enter the RX and some of it would be reflected towards the TX. The reflected energy would return to the TX and would again be partially reflected toward the RX, and then again to the TX, then RX, etc. This back-and-forth reflection is what this work refers to as reflection activity.

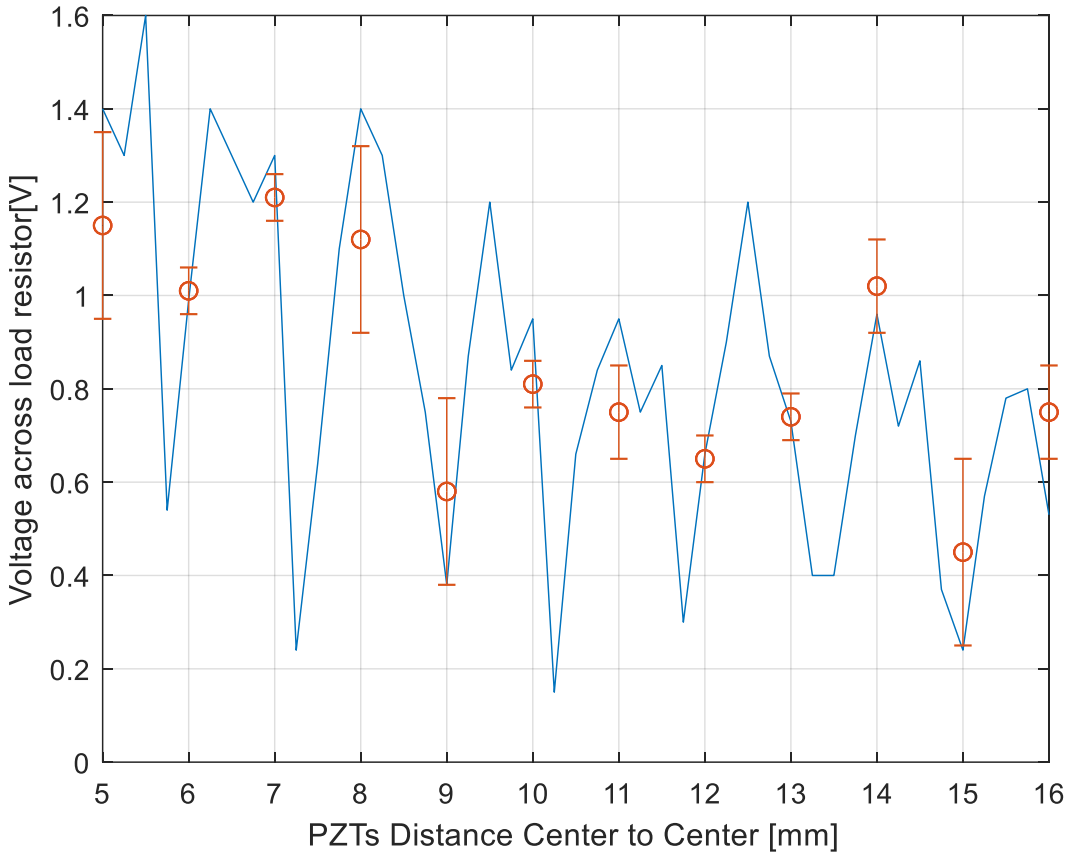

Figure 29: PZT-4, TX-diameter= 10 mm & RX-diameter= 21 mm. The thickness for TX and RX is 2.07 mm, the distance between PZTs is changed.

Figure 30 shows a small power transfer efficiency starting at 1 %. This efficiency decreases with an increase in distance to reach almost zero power transfer at 16 mm. The efficiency is fluctuating, due to the intrinsic near field oscillations.

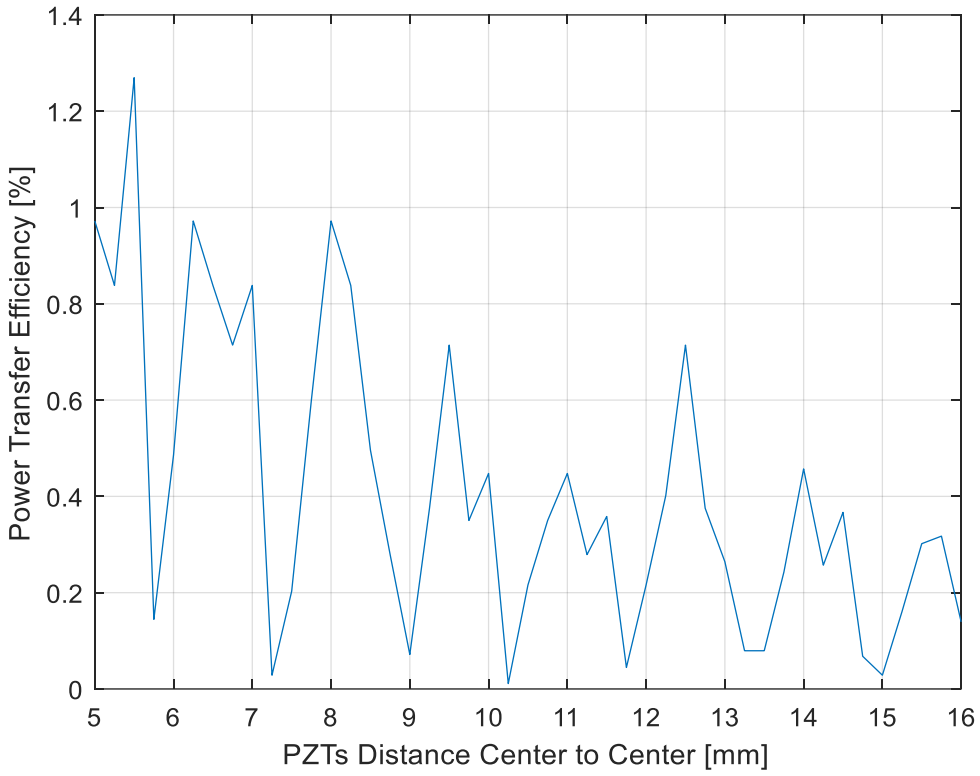

Figure 30: Power transfer efficiency as a function for the distance between the TX and RX, RX is bigger diameter than TX.

The input and output voltages and the experimental setup are presented in figure 31. The Vpp is equal to 14.1 V.

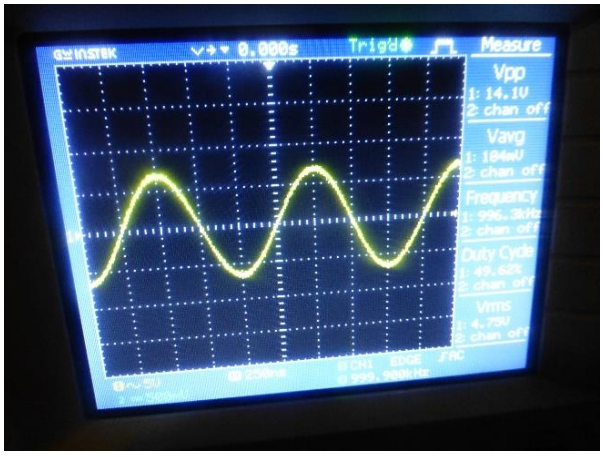

Oscilloscope measure the input voltage for TX.

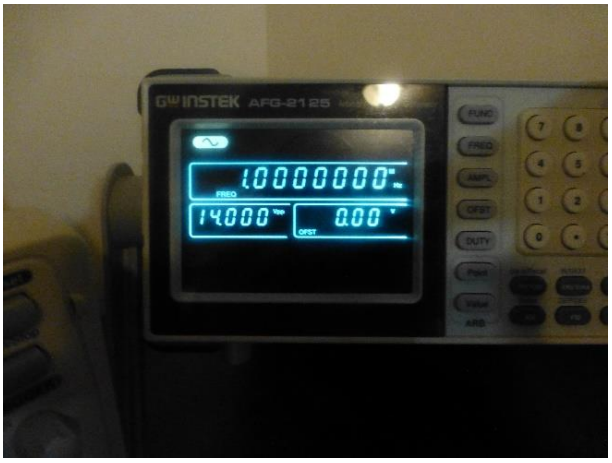

Function generator the frequency is 1 MHz and amplitude equal to 14 Vpp.

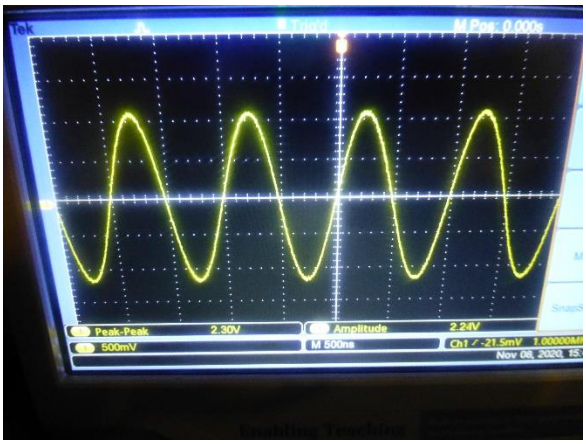

The output voltage peak-peak at 2.30 V.

Figure 31: Experimental setup when TX and RX have different diameter.

In figure 32 the PZT receiver has the same diameter (10 mm) as the transmitter. A comparison of figures 32 and 23 shows that when the coupled PZTs' diameters are smaller, more energy will be lost by the system. One reason for this is the higher impedance associated with smaller PZT diameter. Another reason is signal attenuation due to beam divergence and absorption in the medium.

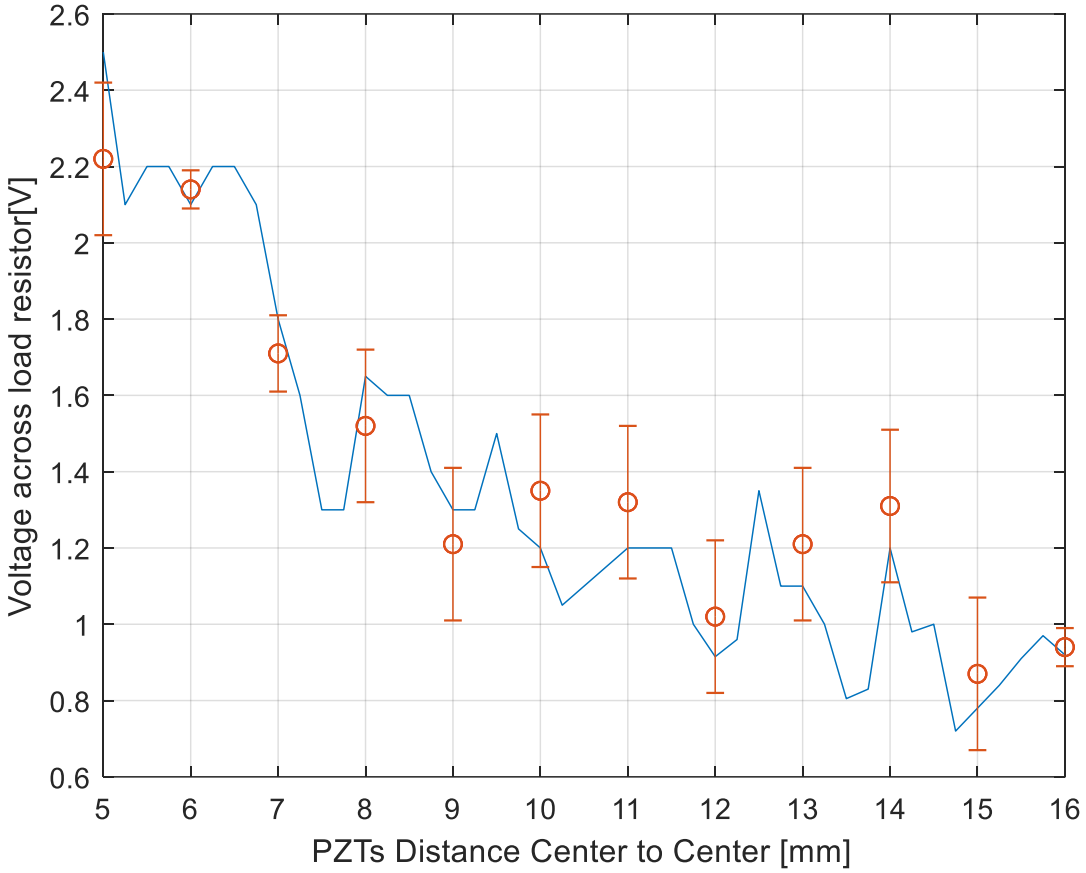

Figure 32: Diameter= 10 mm for RX & TX, the PZTs thickness is 2.07 mm. The voltage across the load resistor as a function for the distance between PZT. The red circle represents the experimental results while the blue line represents the simulation results.

Figure 33 shows how the power transfer efficiency decrease by changing the distance between the PZT system. The shape of figure 33 compares to figure 32 looks compatible but, the value is different. This system generates efficiency equal to 3% but it is higher than the system in figure 30. However, this efficiency falls off with distance much faster.

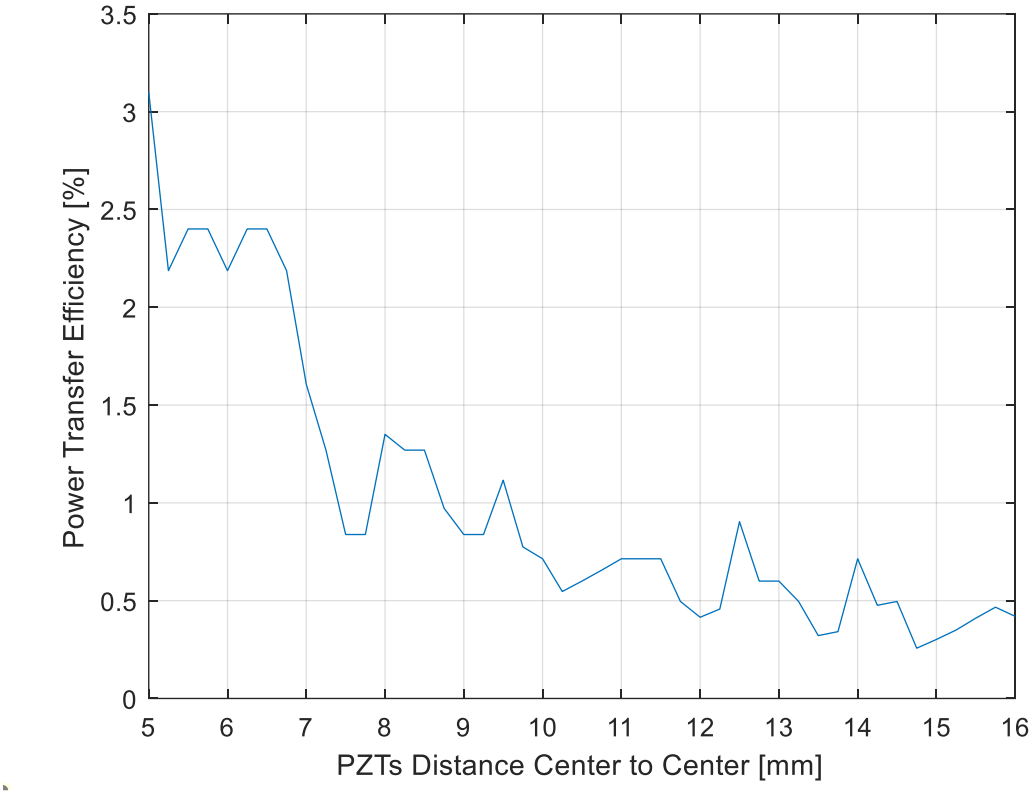

Figure 33: Distance between PZT as a function for power transfer efficiency when diameter= 10 mm for RX & TX.

The output voltage and the experimental setup are presented in figure 34. The Vpp is equal to 14.1 V.

Function generator the frequency is 1 MHz and amplitude equal to 14 Vpp.

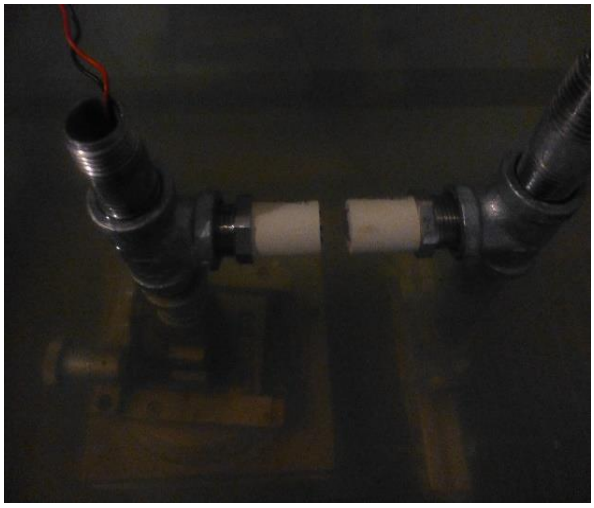

PZT TX and RX inside the aquarium.

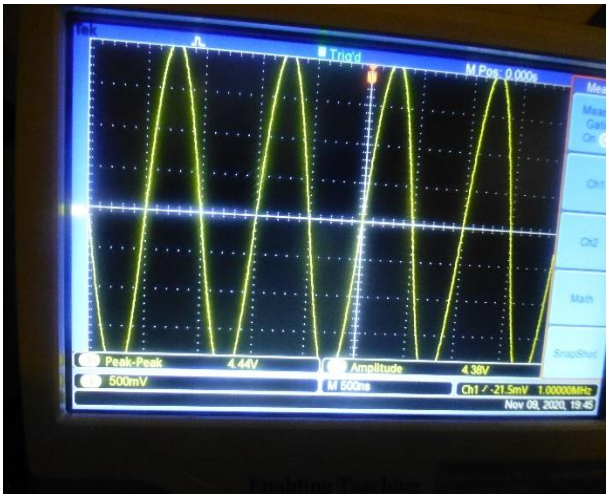

The output voltage peak-peak at 4.44 V.

Figure 34: Experimental setup when TX and RX have the same diameter of 10 mm.

5.3 Effects of key factors on power transfer efficiency

Calculation of power transfer efficiency is an essential tool for ensuring successful system design. Figure 35 shows that the distance between the TX and RX of the PZT plays an important role in the percentage of input power that is dissipated in the load as output power. The maximum calculated power transfer efficiency was more than 12% at a frequency is 900 kHz, which is not the system's natural frequency.

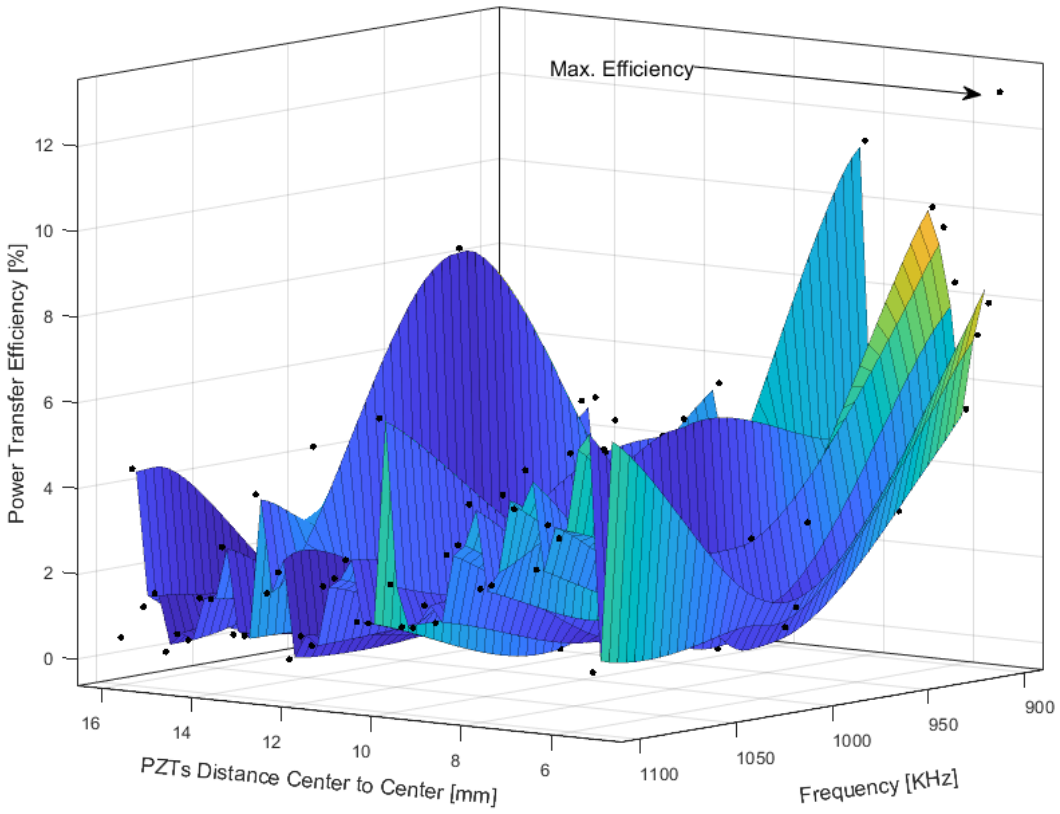

Figure 35: Power transfer efficiency as a function for distance and frequency, the PZT thickness is constant and equal to 2.07 mm.

However, the efficiency depends on the size, structure, physical spacing, relative location, and properties of the environment surrounding the PZT [3].

Figure 36 shows the voltage generated in the resistance load as a function of the separation and thickness of PZT transducers when they operate at their natural resonance frequency. The natural frequencies are 2.07, 1.04, and 0.69 MHz at a thickness equal to 1, 2, and 3 mm, respectively. The thickness and diameter of TX and RX are equal in these calculations. In the figure a calculated voltage near 10 V at a thickness equal to 1 mm and small separation is shown. Whatever the

frequency or the thickness values, the distance between PZT is the most important factor in the output voltage due to the large oscillation in the near field region.

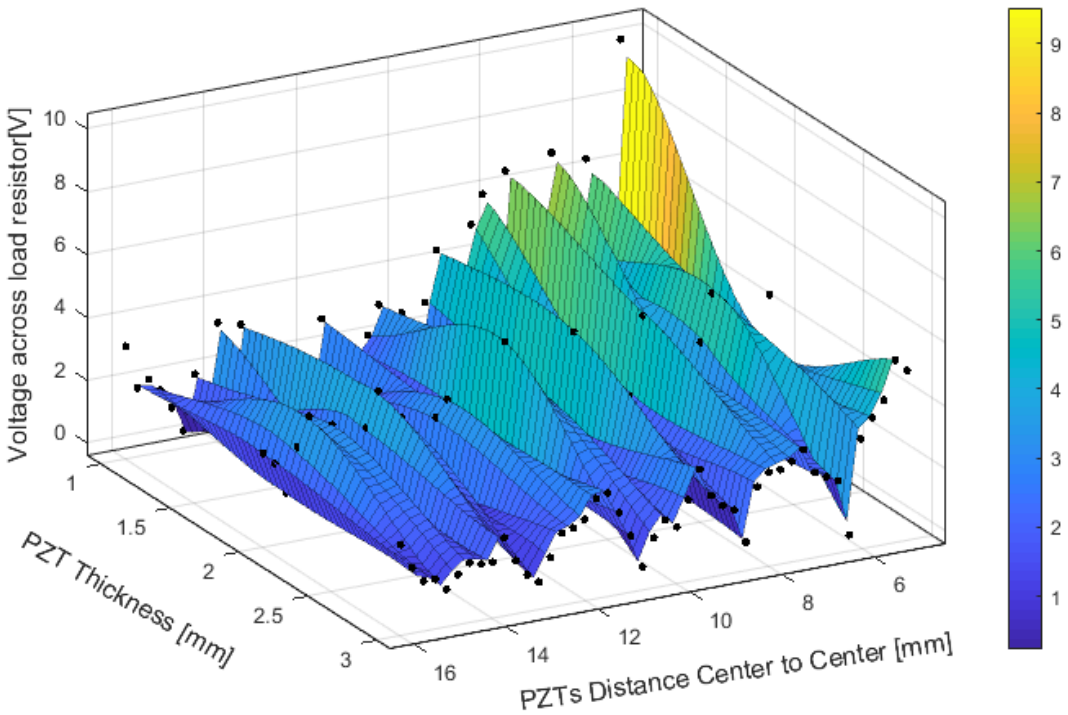

Figure 36: Voltage across load resistor as a function of thickness and skin depth at the resonance frequency of the PZT.

In applications where the TX orientation is not fixed, a slight change in the TX angle can result in a reduction in voltage delivered to the load. The motion of TX in figure 37 is like a pendulum. The figure shows a rapid decrease in the voltage between 0 and 2 degrees but when the TX angle is increased to reach 3 degrees the voltage is almost as large as at zero degrees. This jump is due to three factors: first, the reflection activity between the TX and RX decreases, second the reflection coefficient at the RX face changed because the transmission line impedance changed, third the pressure profile on the RX face changes.

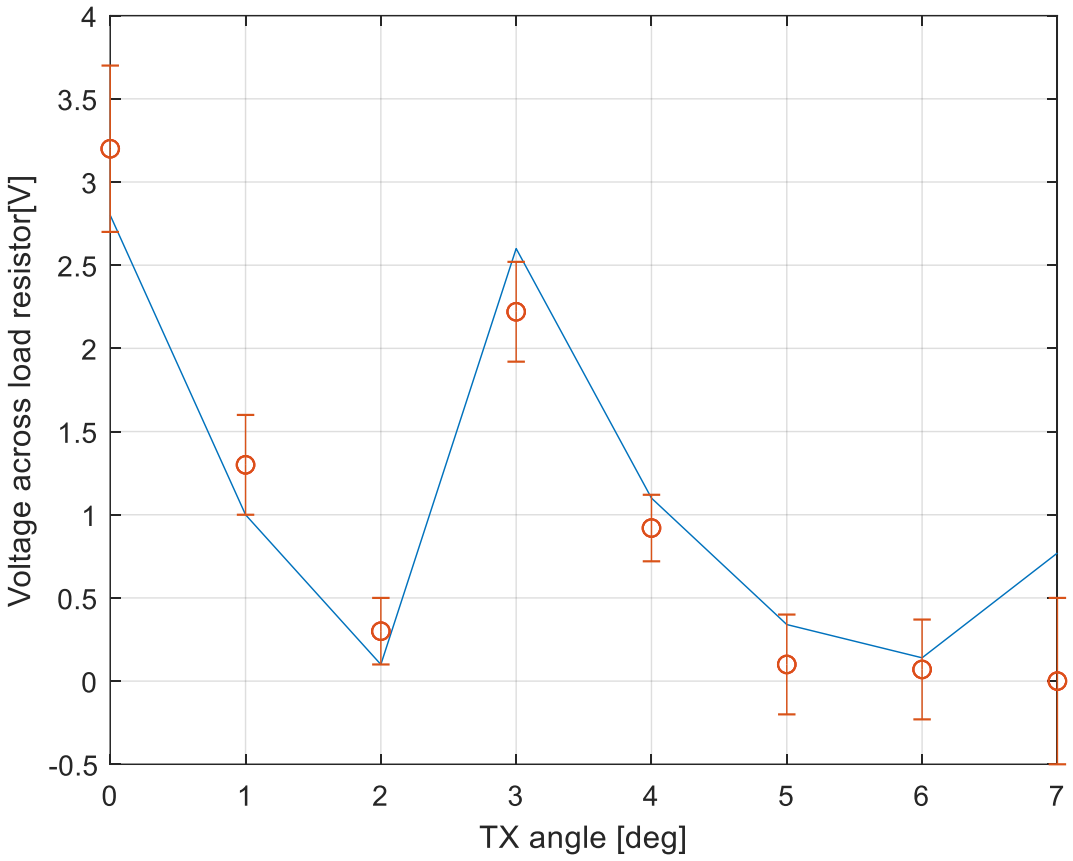

Figure 37: TX diameter 21 mm, RX diameter 10 mm. RX and TX thickness is 2.07 mm. The distance between RX and TX is 10 mm. In this case, there rare two types of motions: offset and orientation together.

Figure 38 shows the power transfer efficiency as a function of the TX angle. The efficiency decreases rapidly since the PZT-TX starts to rotate to reach 0% at two degrees. The efficiency starts to increase to reach 3.3% at 3 degrees, this increment because the acoustic wave could be compatible with the angle of rotation.

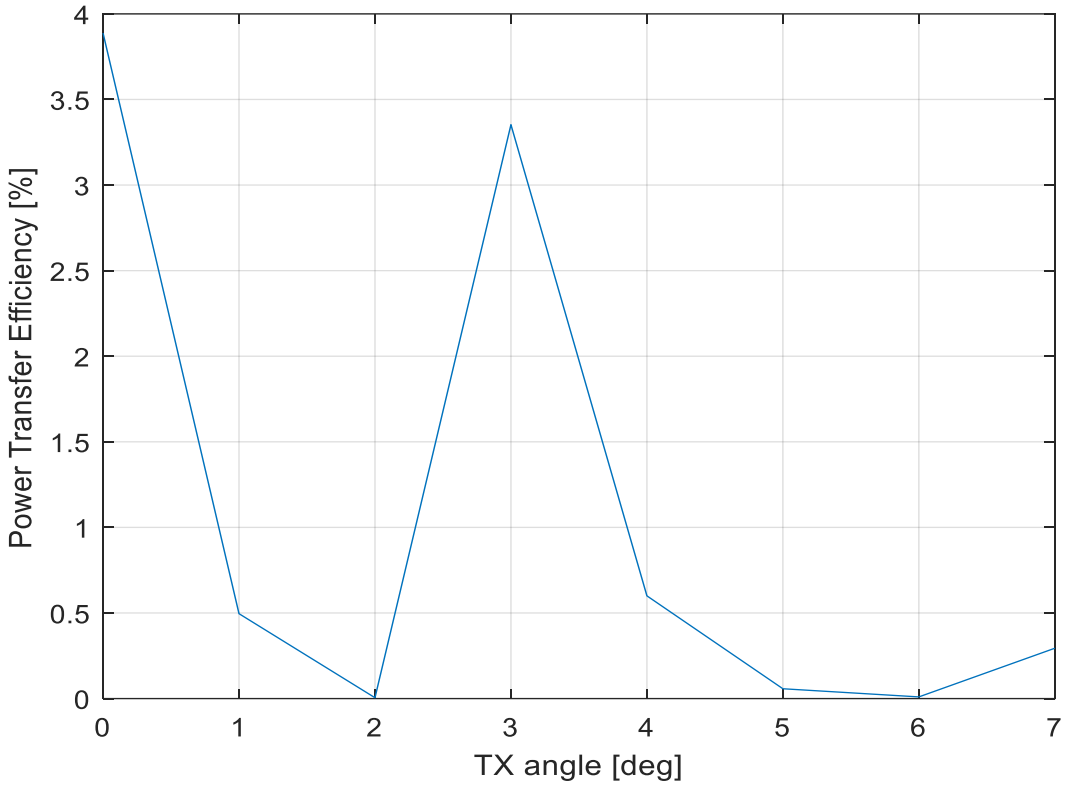

Figure 38: Power transfer efficiency vs. TX rotation angle. TX diameter 21 mm, RX diameter 10 mm. TX diameter is bigger than that of the RX.

Figure 39 shows that when the TX is smaller than RX (TX diameter 10 mm, RX diameter 21 mm), as in figure 37, the voltage generated will be less. When the angle increased a rapid loss of the voltage is observed. This figure is created by measuring load voltage as the angle is varied for a fixed depth and zero offsets. It can be said that with a decrease in the TX diameter less energy will be generated.

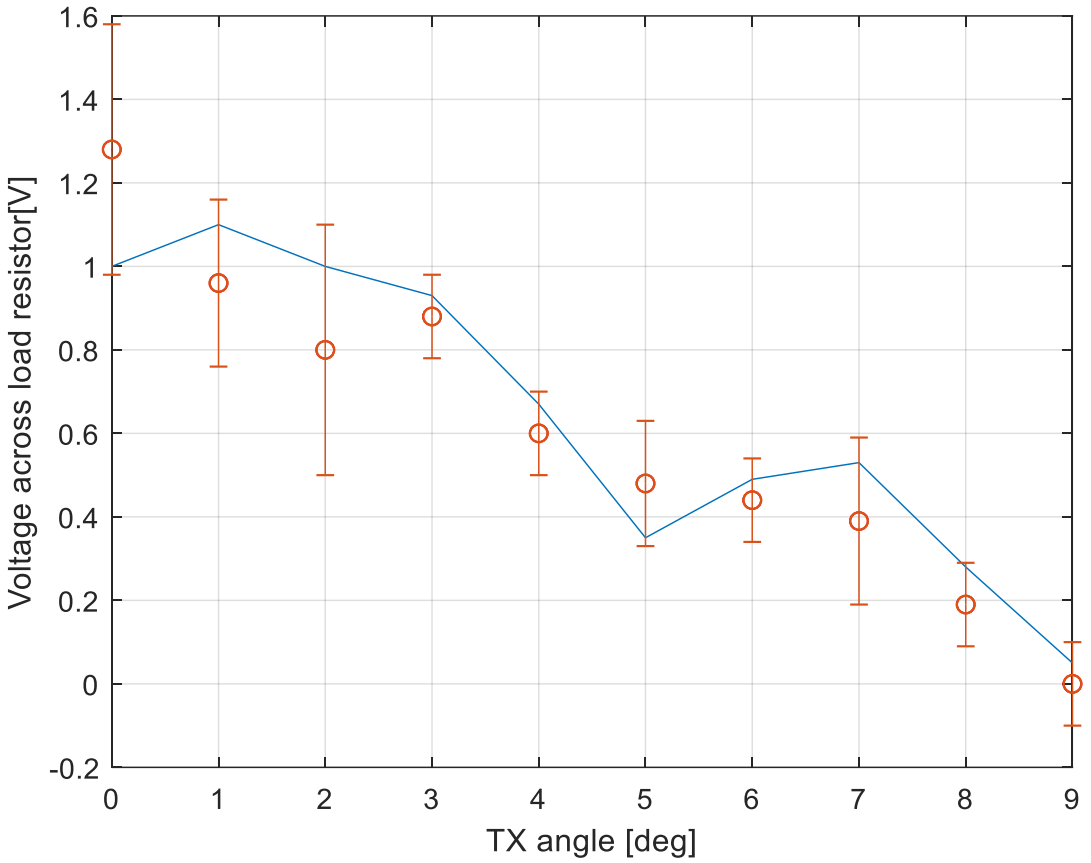

Figure 39: TX diameter 10 mm, RX diameter 21 mm, the red circle is the experimental result, the blue line represents the theoretical results, and the vertical red line represents the error bar. TX and RX thickness of 2.07 mm.

Figure 40 shows a low calculated power transfer efficiency that starts at 0.5%, raises a little at 1 degree, drops to zero% at 9 degrees. This figure indicates that increasing the PZT-TX angle will decrease system efficiency.

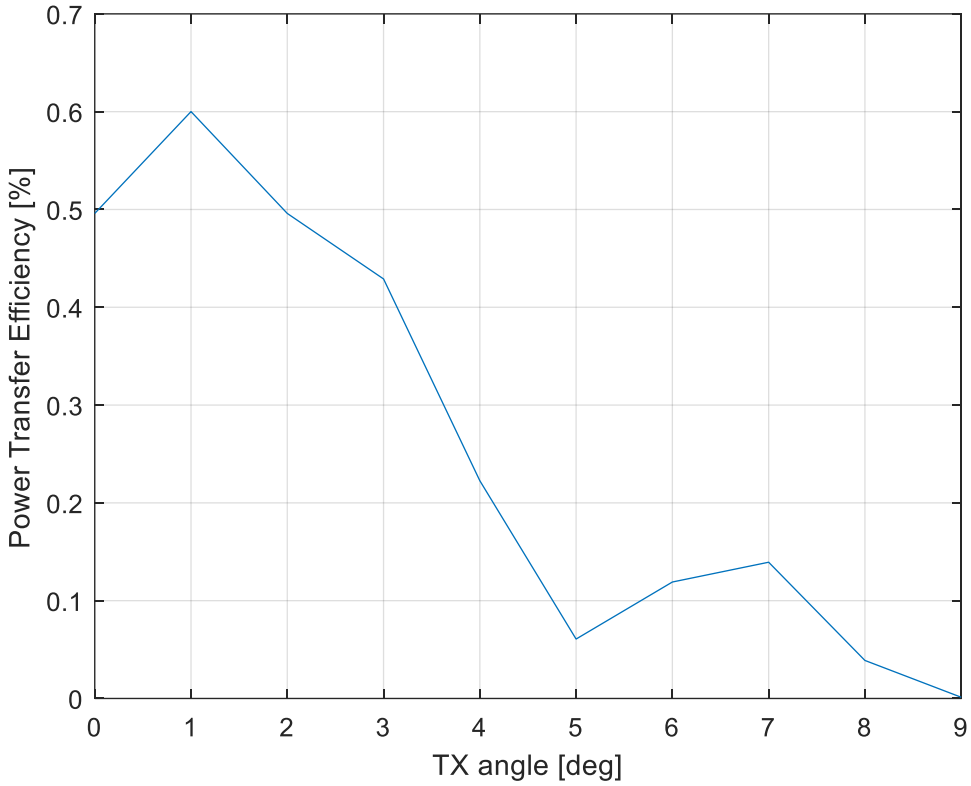

Figure 40: Power transfer efficiency vs. TX rotation angle, when RX diameter is bigger than that of TX.

Figure 41 illustrates the effect of rotation angle on the voltage created at the RX, where TX is rotated about its center. The acoustic wave generated from the TX has a sinusoidal shape that has a peak and zero value. The PZT voltage value is changing depending on the location of RX and its angle. When the PZT location causes a high peak of power transfer efficiency, the voltage will be high also. The sinusoidal wave has an angle change with distance and time, this angle could be coincidental with the rotation angle of RX and that will result in creating a voltage in the PZT-RX.

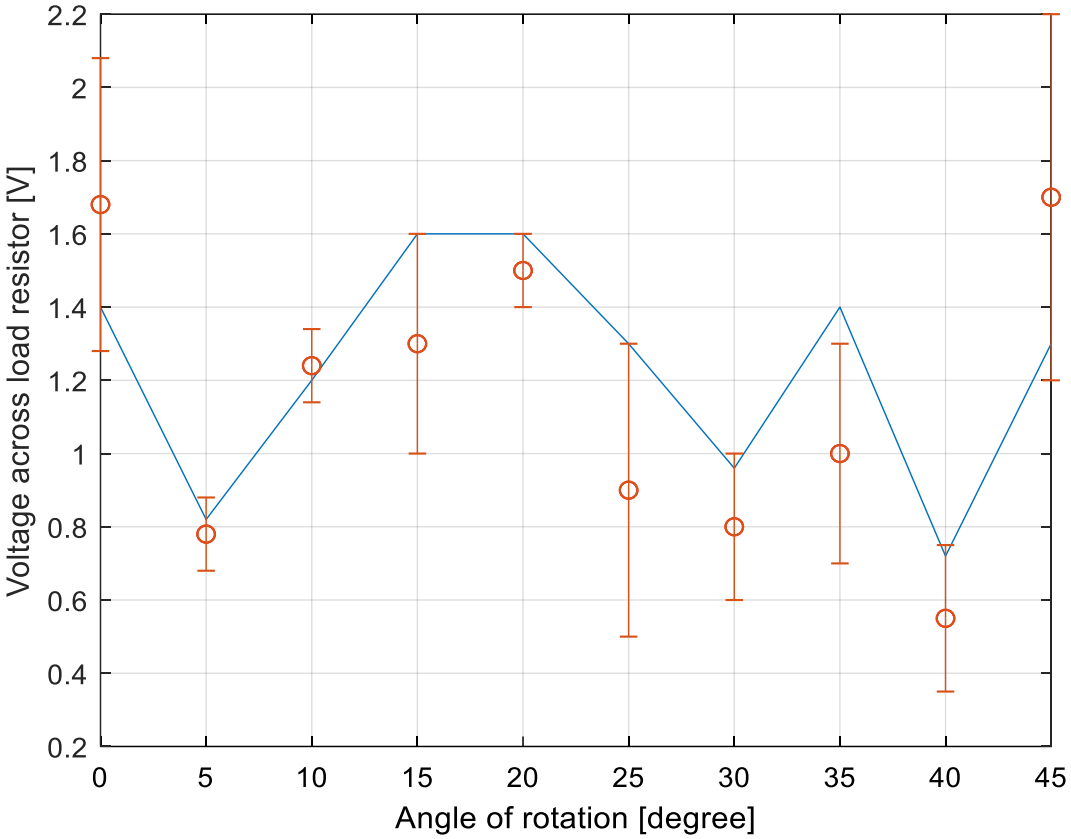

Figure 41: TX rotates about its center and the distance between TX and RX stays constant at 16 mm. TX and RX diameter and thickness are 21 mm and 2.07 mm, respectively. The distance between TX and RX is 16mm.

Figure 42 shows a peak power transfer efficiency at an angle of 15 degrees, this peak continues constantly until the angle of 20 degrees. The motion of the PZT-TX in this figure is a compound of rotation and translation at the same time. The PZT-RX during this movement comes close to the PZT-TX and that is why we get this peak there.

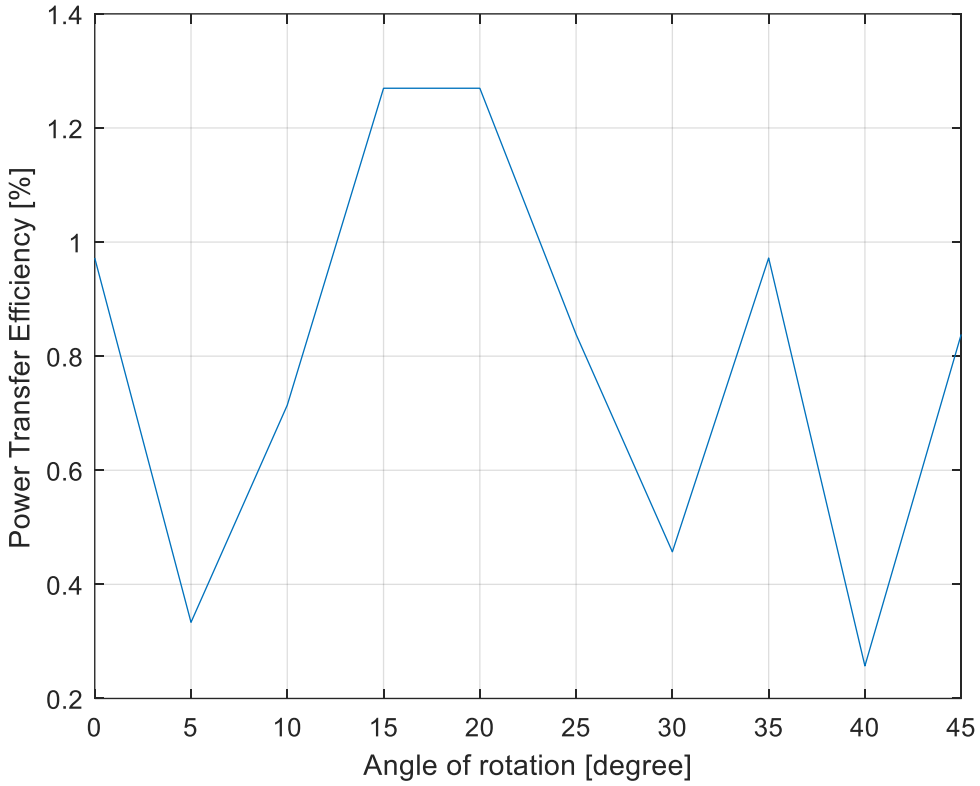

Figure 42: Power transfer efficiency vs. TX rotation angle. TX and RX diameter are 21 mm, the thickness is 2.07 mm. The distance between TX and RX is 16 mm.

5.4 Summery of power transfer with alignment, diameter, and thickness

The power transfer efficiency can be multiplied when the RX and TX diameters duplicate. This does not mean that increase in the diameter of RX or TX alone will increase efficiency, but it could decrease it. There is also a notice that when RX is smaller than TX, the power efficiency is higher than when TX is bigger than RX. The system can lose its power transfer efficiency significantly when there is even a small rotation angle between TX and RX.

5.5 References

1. DeAngelis, D. A., & Schulze, G. W. (2016). Performance of PZT8 versus PZT4 piezoceramic materials in ultrasonic transducers. Physics Procedia, 87, 85-92.

2. Christensen, D. B. (2017). Acoustic power transfer system for implantable medical device: modeling technique and analysis (Doctoral dissertation, The University of Utah).

3. Ram Rakhyani, A. (2010). Design of efficient wireless power-transfer system and piezoelectric transducer for sonoporation-based drug delivery implants (Doctoral dissertation, University of British Columbia).

CHAPTER SIX: Reflector layer effects on power transfer efficiency

6.1 Introduction

The wave reflection between TX and RX through the medium and the desire to get higher power transfer efficiency opens the gate to discuss how to match the acoustic impedance to the medium. The solution to the reflection problem could be by using a reflector layer. The reflector layer consists of a piece of material that is attached to the RX or TX. The thickness of the reflector layer could be a quarter-wavelength thick [1]. In this chapter, the glue of the reflector layer to the PZT will be negligible because the glue layer has negligible thickness compared to the reflector layer thickness [1]. In the case of multiple reflector layers required, the thickness of the gluing layers will be effective and necessary to calculate [2]. Titanium and Graphite consider a good reflector layer because they are compatible with medical applications.

6.2 Effects of material and dimension

Figure 43 shows how the calculated power transfer efficiency changes as the thickness of the reflector layer changes. The reflector layer has been installed in the back of the PZT transmitter and receiver. Both thicknesses change by the same amount. It can be observed from the results that increasing the thickness of the back layer can increase efficiency. The frequency used in these calculations is 1 MHz. The results show two interesting peaks, one for the titanium at 2.75 mm and a second for the graphite at 2.25 mm, with voltages of 10 V and 8.25 V, respectively. The titanium, as a reflector layer, can increase the transfer efficiency to 50%.

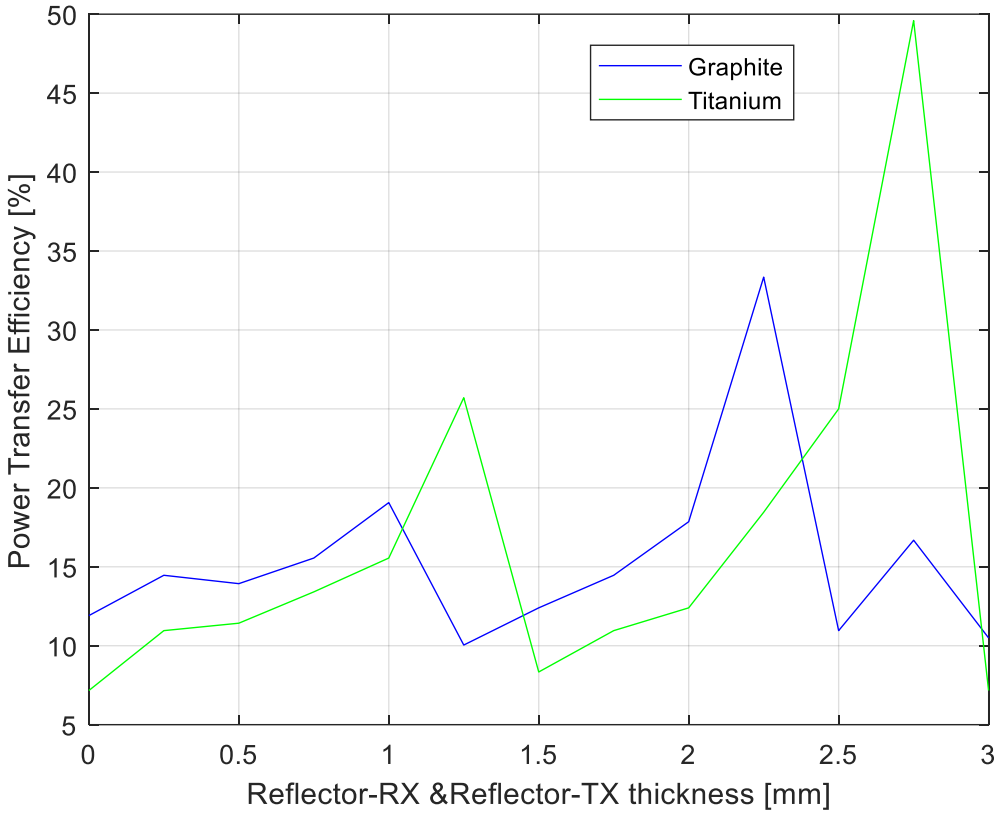

Figure 43: Changing the thickness of the reflector layer attached to PZT-RX as a function of power transfer efficiency. The diameter for TX, RX, and reflector equal to 21 mm.

Figure 44 shows how calculations of power transfer efficiency change as the reflector thickness changes. In this case, the reflector is attached to the back of PZT-RX only. The frequency used is 1 MHz. When the thickness of titanium is 1 mm, we get an increase in the power efficiency to 35%. There are two peaks in figure 44, at 0.5 mm thickness for graphite and 1mm thickness for titanium.

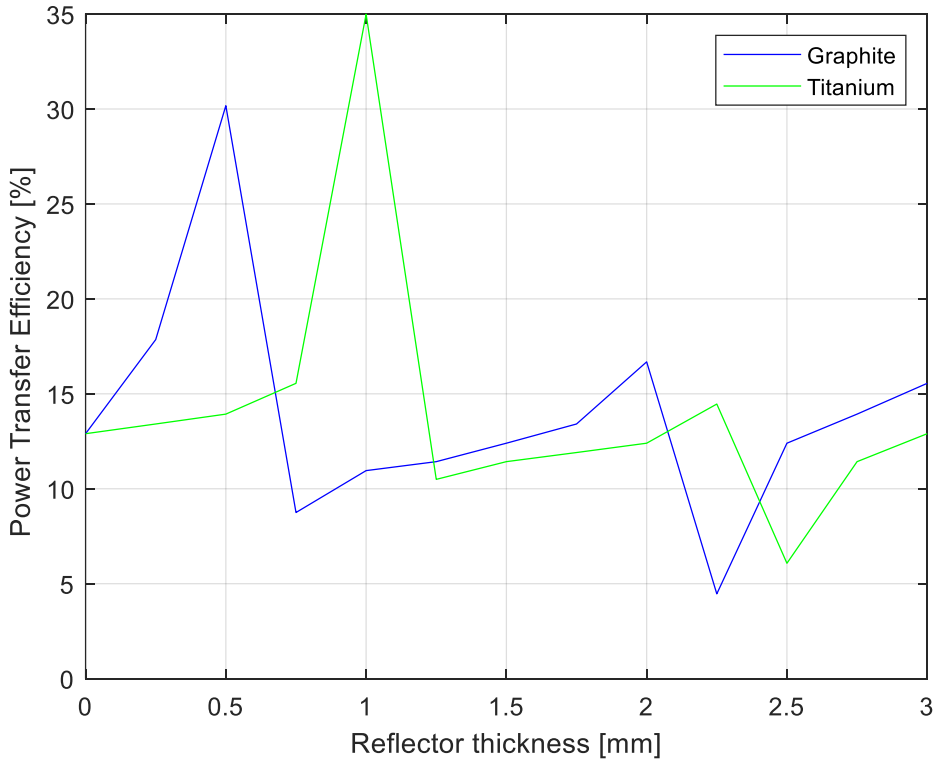

Figure 44: Reflector layer attached to RX, changing the thickness of reflector, as a function of power transfer efficiency. Distance between the reflector and TX is 1 mm.

Figure 45 shows how calculations of transfer efficiency change when the distance between the PZT-RX and the reflector increases. The thickness of the PZT RX, TX, and reflector is equal to 2.07 mm and the diameter of all three components is 21 mm. From the figure, increase the distance leads to an increase in power transfer efficiency. At zero distance between RX and reflector the power transfer efficiency equals 1% for titanium. Increase the distance shows many peaks and null until the power efficiency reaches 25% in the titanium case. This increment caused by reflector is due to the work of the reflector as a concave lens for the acoustic wave and return the wave to the PZT RX to switch it to voltage again. The graphite shows a peak at 1 mm but it returns approximately to the same power efficiency at a distance of 3 mm.

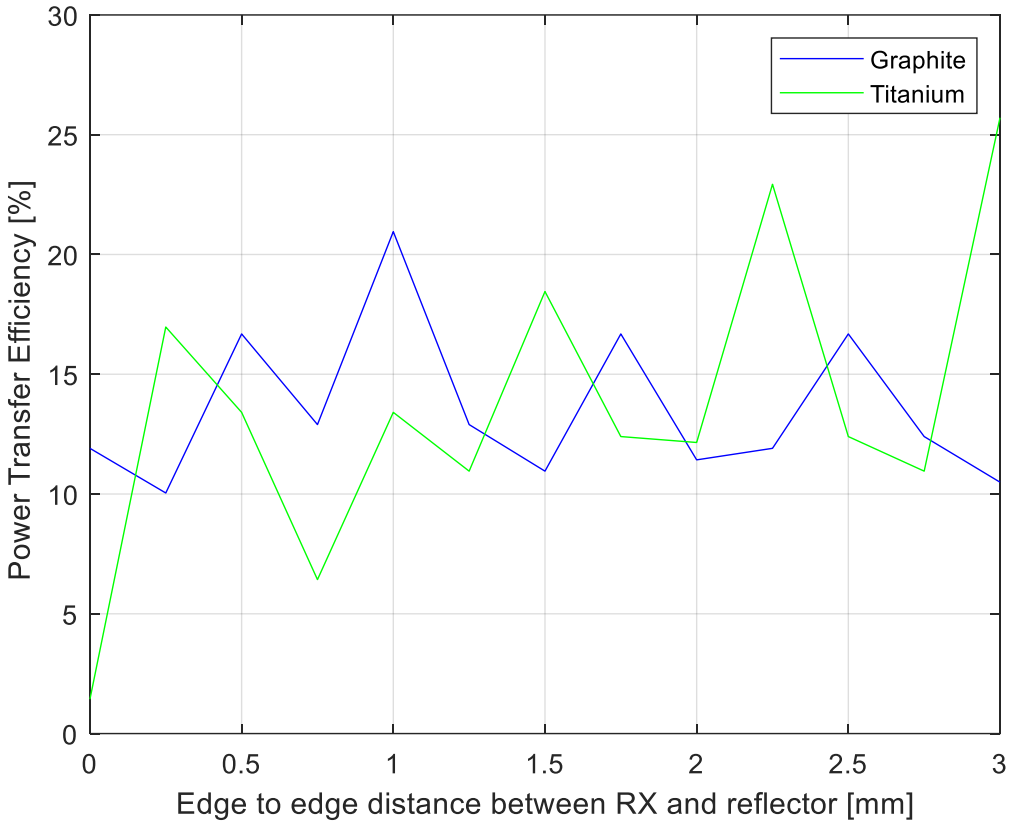

Figure 45: Distance between RX and reflector as a function of power transfer efficiency. PZT-RX, TX, and reflector thickness equal to 2.07 mm, diameter equals to 21 mm.

Figure 46 shows the dependence of calculated power transfer efficiency on the diameter of the refector behind RX. Reflector, RX, and TX have the same thickness of 2.07 mm. The frequency is 1 MHz. The separation of RX and reflector is 1 mm. Both materials show the same increase in power transfer efficiency until the diameter equals 0.85 mm. Then the curves diverge with titanium showing no increment in the power transfer efficiency, while the graphite is affected significantly by the change of reflector diameter between 3 and 25 mm.

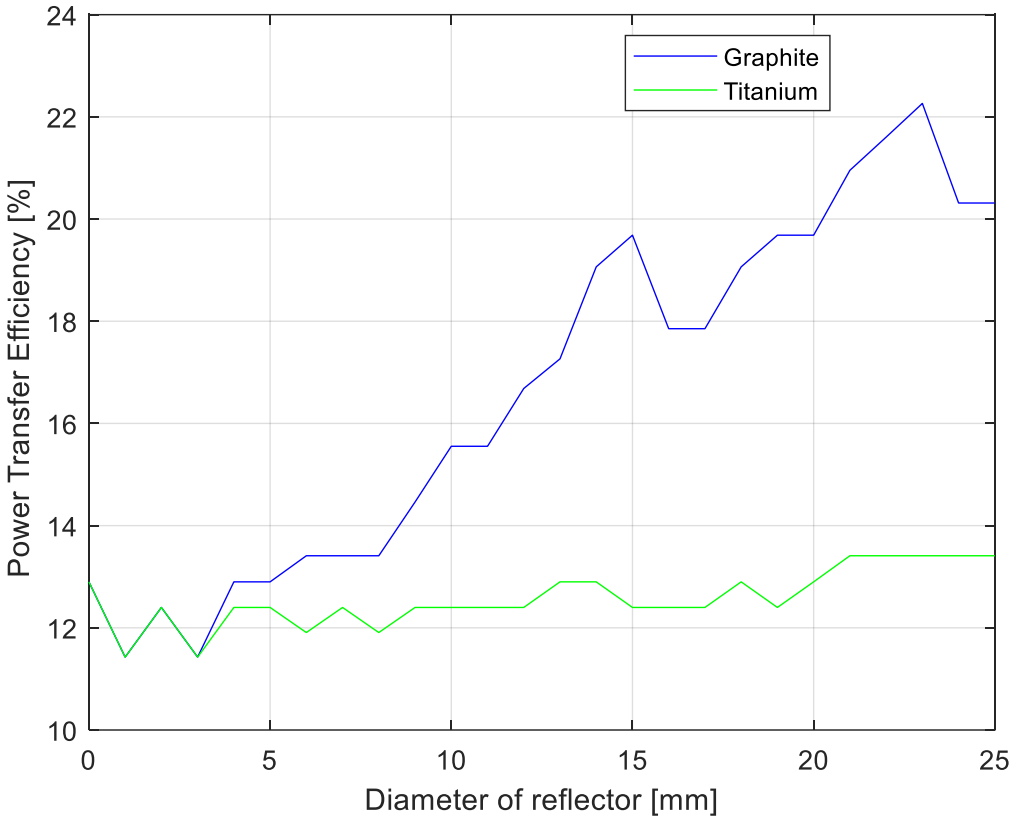

Figure 46: Diameter of reflector as a function of power transfer efficiency, the thickness of reflector, RX, and TX equals 2.07 mm. RX and TX diameter equals 21 mm. The distance between RX and reflector is set to 1 mm.

6.3 Four reflectors

The simulation of sound pressure level shown in figure 47 was done by using four graphite reflectors, one in front and one in the back of TX and the same for RX. The distance between the PZT center to center is 5 mm. The thickness of each PZT is 2.07 mm. The thickness of each reflector layer is 0.5 mm. The distance between the reflector and RX face or TX is 0.125 mm. Figure 47 shows that the highest sound pressure (red color) is kept between the faces of the PZT.

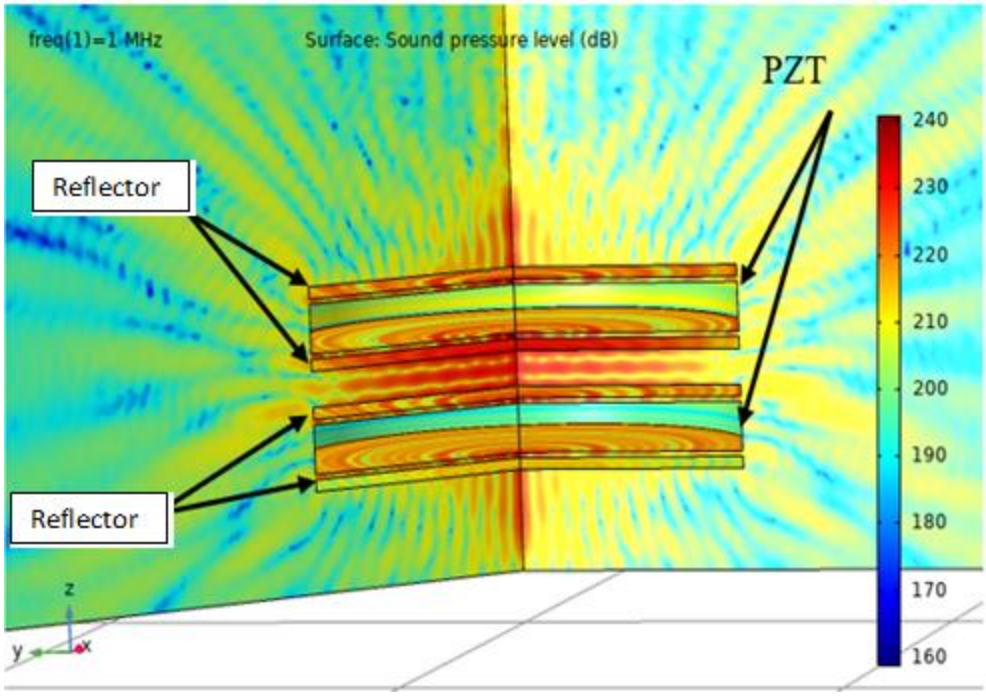

Figure 47: Sound pressure level with four reflectors.

Figure 48 illustrates how the efficiency of using four reflectors changes as a function for reflector diameter. Comparing figure 48 with figure 46 that has only two reflectors shows that at 25 mm diameter, for example, increase the efficiency from 20% to 45%. Comparing to figure 43 at a reflector thickness equals 0.125 mm, it can show that the four reflectors increase the efficiency from 15% to 50%.

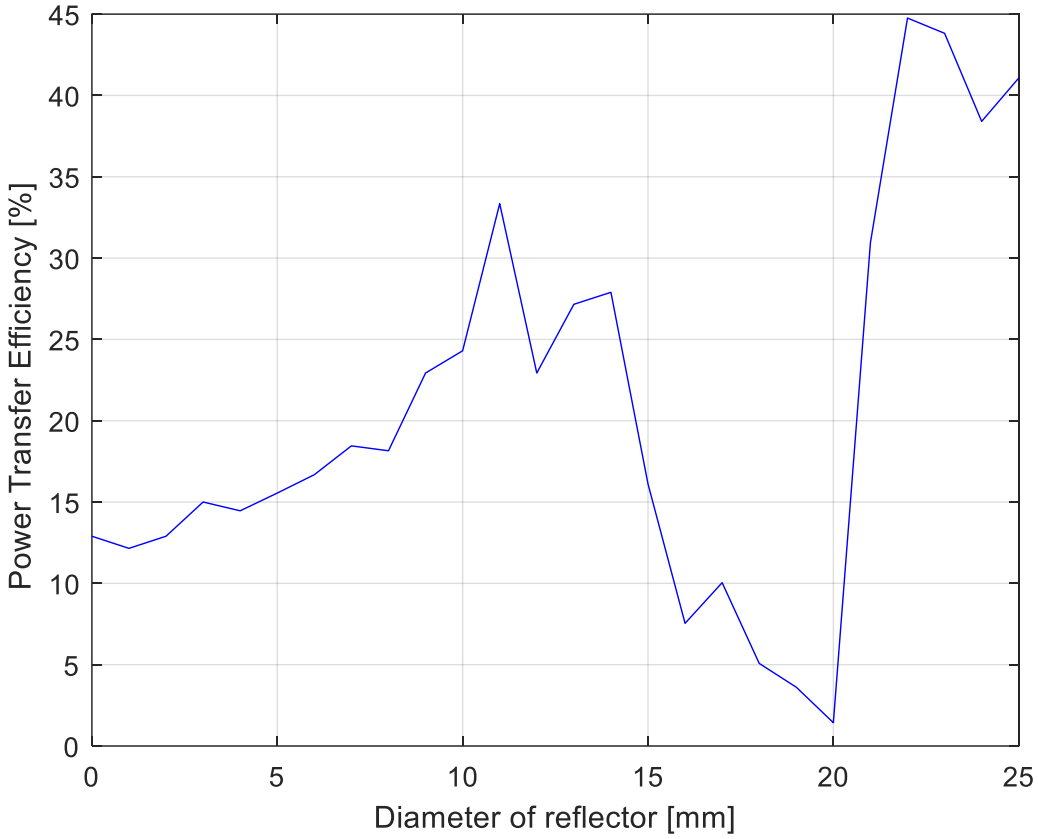

Figure 48: Power transfer efficiency as a function of four reflectors. TX and RX diameter are 21 mm and the thickness is 2.07 mm. Reflector thickness is 0.5 mm. The distance between the face of the reflector and the face of RX and TX is 0.215 mm.

6.4 Summary of reflector layer effects on power transfer efficiency

The power transfer efficiency shows how the reflector layer can improve system efficiency. Changes in the diameter, thickness, and location of the reflector make the power transfer efficiency higher. The reflector layer reflects the acoustic wave and return the wave to the PZT, working as a lens.

6.5 References

1. Christensen, D. B. (2017). Acoustic power transfer system for implantable medical device: modeling technique and analysis. (Doctoral dissertation, The University of Utah).

2. Callens, D., Bruneel, C., & Assaad, J. (2004). Matching ultrasonic transducer using two matching layers where one of them is glue. Ndt & E International, 37(8), 591-596.

CHAPTER SEVEN: Conclusion and recommendation

7.1 Conclusion

Acoustic power transfer for medical devices is showing progress on miniaturization. Among different transduction mechanisms, piezoelectric transduction seems to be more attractive since it can produce devices capable of generating higher power densities compared to electrostatic transduction. Although the piezoelectric plate structure can provide the required power for most implantable devices, the voltage and power delivered to the load from the TX is a function of RX position (depth, orientation, and alignment relative to the TX), frequency, TX, and RX diameter, and source and load impedance. To accomplish this purpose, simulation data is analyzed dimensionally and compiled into design graphs to provide insight into voltage and power sensitivity to system parameters.

In complex systems like the near-field region of a piezoelectric energy transfer system, simulation can be an efficient method to understand system efficiency. To be effective, simulation methods must be experimentally validated. In this work, it is shown that selected predictions of the COMSOL simulation results for the output voltage of a piezoelectric device are consistent with experimental measurements. Even though more experiment validations are desirable, the results presented in this works give us confidence in the use of COMSOL for the design of an ultrasonic piezoelectric power transfer system. The simulations suggest that the diameter of the receiver should be less than the diameter of the transmitter, perhaps as much as 50%. They also indicate that system performance will degrade rapidly for frequencies below 1 MHz.

Reflector layers were explored in this work and simulation analysis showed that the reflector layer can improve power transfer efficiency depending on its material, dimension, and location.

7.2 *Recommendation*

1. Study the relation between the mechanical quality factor of different PZT with the power transfer efficiency. This can help to see if there is any relation between changing the PZT thickness and the mechanical quality factor.
2. Use a different couple of PZT for sending and receiving the signal. The fundamental frequency of each PZT and the mechanical impedance will be different than others. This could lead to understanding the relationship between the frequency and the generated power transfer efficiency.
3. Comparison of adding a different type of reflector layer for the same PZT couple. This can help to study the effect of different sizes of PZT diameter with different reflector layer. It can be studied the effect of a couple of parameters on power transfer efficiency.
4. Focus more on the reflector layer and the design shape of the piezoelectric material to improve the power transfer efficiency. Instead of using one PZT to provide the ultrasound, the use of an array of piezoelectric transducers is suggested. This may overcome the problem of misalignment.
5. Use the motor instead of hand in the experiment to get a more precise measurement. This will help to follow the value of the near-filed and find the highest acoustic pressure point to install the PZT at it. This will help to get high power efficiency instead of increasing the system frequency and generate a high-temperature effect on the skin of the human body.